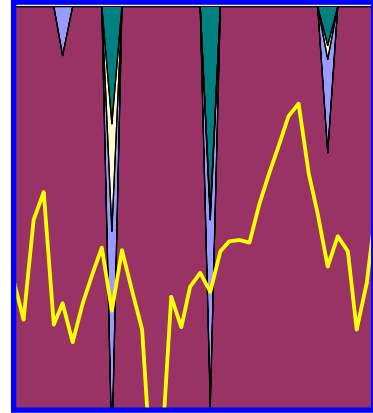
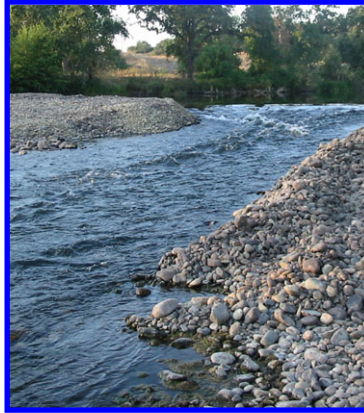
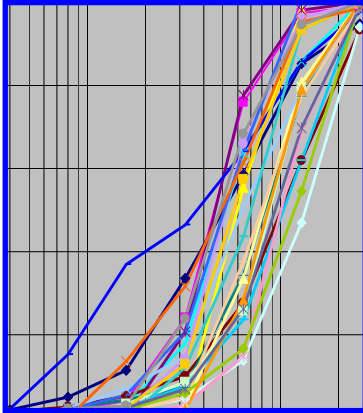


Merced River Corridor Restoration Plan
Phase IV: Dredger Tailings Reach



Technical Memorandum #3
**Sediment Transport Model of the
Merced River Dredger Tailings Reach**

Prepared for
CALFED ERP
Sacramento, California
Recipient Agreement No. ERP-02-P12-D

Prepared by
Stillwater Sciences
2855 Telegraph Avenue, Suite 400
Berkeley, California 94705

May 2004

For more information or copies of this Technical Memorandum, please contact:

Stillwater Sciences
2855 Telegraph Avenue, Suite 400
Berkeley, CA 94705
stillwatersci.com
(510) 848-8098

Suggested citation: Stillwater Sciences. 2004. Sediment transport model of the Merced River Dredger Tailings Reach. Stillwater Sciences, Berkeley, California.

Table of Contents

1	INTRODUCTION	1
	1.1 Project Setting.....	1
	1.2 Project Overview and Objectives	4
2	GOVERNING EQUATIONS AND SOLUTION TECHNIQUE.....	9
3	INPUT PARAMETERS	15
	3.1 Hydrology	15
	3.2 Longitudinal Profile and Cross-sections	15
	3.3 Surface Grain Size Distributions	16
	3.4 Coarse Sediment Supply.....	17
	3.5 Gravel Augmentation and Wing Dams	18
4	ZERO PROCESS AND SIMULATION OF BACKGROUND CONDITIONS PRIOR TO GRAVEL AUGMENTATION	21
5	EVALUATION OF CURRENT CONDITIONS	25
6	CONCLUSIONS AND DISCUSSION	27
7	REFERENCES	29
8	FIGURES.....	33

LIST OF TABLES

Table 3-1. Amount of gravel augmentation at the upstream end area of the Dredger Tailings Reach.	18
Table 4-1. An arbitrary definition of channel bed mobility according to the normalized Shields stress ϕ_{sgo} in the surface-based bedload equation of Parker (1990), where the description of each bed mobility stage is rather speculative.....	22

LIST OF FIGURES

Figure 1. The Merced River Dredger Tailings Reach, showing locations of channel cross-section surveys, pebble counts, and wing dams.	
Figure 2. Simplified channel cross-section and definition of geometric parameters.	
Figure 3. Daily average discharge record at the Merced River below Merced Falls Gauge (USGS # 11270900) for the post-New Exchequer Dam period between 10/1/1972 and 9/30/2002.	
Figure 4. Longitudinal profile of the Merced River Dredger Tailings Reach. Interpolated bed elevations are based on KSN, Inc. survey data.	
Figure 5. Simplification of surveyed channel cross-section.	
Figure 6. Pebble counts in the Merced River Dredger Tailings Reach.	
Figure 7. Characteristic grain sizes in the Merced River Dredger Tailings Reach.	
Figure 8. Gravel wing dam #4 on the Merced River within the Dredger Tailings Reach.	
Figure 9. Estimated grain size distribution of gravel used at the Merced River Hatchery augmentation riffle.	
Figure 10. Sketch demonstrating the longitudinal distribution of augmented sediment as a gravel pulse.	
Figure 11. Simulated thickness of sediment deposit for a 30-year period plotted annually.	
Figure 12. Simulated surface median size for a 30-year period plotted annually.	
Figure 13. Annual run-off for the post-New Exchequer Dam period between water years 1973 and 2002.	
Figure 14. Daily discharge record for water year 1983.	
Figure 15. Simulated bed mobility for water year 1983 in comparison with (a) river longitudinal profile; and (b) surface median grain size.	
Figure 16. Simulated thickness of sediment deposit with the ongoing gravel augmentation before 9/30/2002.	
Figure 17. Simulated surface median grain size with the ongoing gravel augmentation before 9/30/2002.	
Figure 18. Bed elevation and surface median size downstream of the hatchery gravel augmentation site approximately 250 m (820 ft) downstream of Crocker-Huffman Dam.	

I INTRODUCTION

The purpose of this technical memorandum is to document the development and results of a reach-scale sediment transport model used to assess sediment mobility conditions within the Merced River Dredger Tailings Reach (DTR). The numerical sediment transport model discussed in this report was developed to examine the current sediment transport conditions and the effectiveness of potential restoration strategies in the DTR, such as narrowing the main channel, re-grading the floodplain, and augmenting gravel, in improving the dynamics (e.g., texture, thickness of deposit, mobility) of the channel bed.

This technical memorandum describes the setting and context for the sediment transport model, the parameters used as input to the model, and the model results under existing channel conditions, specifically:

- *Governing equations and solution technique.* Governing equations for flow, grain size, and overall transport capacity were reviewed and updated to include floodplains in the sediment transport model.
- *Analysis of input parameters.* Flow data from gauging stations in the DTR, longitudinal profile and cross-section surveys, pebble count data, coarse sediment supply data, and mass of introduced gravel from constructed wing dams and gravel augmentation projects were reviewed for model input.
- *Zero process and simulation of background conditions prior to gravel augmentation.* Model output is provided for assumed sediment supply under background conditions.
- *Evaluation of current conditions.* Model output is provided for gravel pulses under existing channel conditions.

This report is the third in a series of technical memoranda that will detail the existing and potential post-restoration physical and biological conditions of the DTR.

1.1 Project Setting

The Merced River is a tributary to the San Joaquin River in the southern portion of California's Central Valley. The river, which drains an

approximately 1,276-square-mile watershed, originates in Yosemite National Park and flows southwest through the Sierra Nevada range before joining the San Joaquin River 87 miles south of the City of Sacramento. Elevations in the watershed range from 13,000 feet at its crest to 49 feet at the confluence with the San Joaquin River. This report focuses on the DTR of the Merced River, which extends from Crocker-Huffman Dam (river mile [RM] 52) to approximately 1.2 miles downstream of the Snelling Road Bridge (RM 45.2) (Figure 1). The channel in this reach is confined by piles of dredger tailings, which have replaced the natural floodplain soils and floodplain forest, and have increased floodplain elevations along the river. Within this reach, riparian vegetation is sparse, occurring primarily in narrow bands along the river channel and in fragmented patches in low-lying areas among the dredger tailings piles.

Historically, this reach was part of a highly dynamic, multiple channel system. Under pre-colonial conditions, as the river exited the Sierra Nevada foothills near Merced Falls, the river spread out across a broad alluvial valley floor that ranged up to 4.5 miles in width (Stillwater Sciences 2001). Within this reach, the historic river was a complex, multiple channel system, including the mainstem river channel and several sloughs. Under pre-colonial flow conditions, the dominant, or “mainstem,” channel likely switched between the multiple channels, and channel avulsions during large flows may have been common.

The hydrology of the Merced River has been altered by water supply requirements and flood control operations, which together have reduced flood frequency, reduced peak flow magnitude, altered seasonal flow patterns, and reduced the temporal variability of flows, spring snowmelt flows, and summer base flows.

Since 1926, sediment supply from the upper 81 percent of the watershed has been intercepted at the original Exchequer Dam and then the New Exchequer Dam. This interception has eliminated the vast majority of the river’s historical sediment supply, thus depriving the river of a basic component in maintaining its existing geomorphic equilibrium and causing a new equilibrium to be sought. With the reduction in flood magnitude caused by flow regulation, the bed is currently immobile at flows up to the 5-year recurrence interval flow (Q_5) (Stillwater Sciences 2001). As a result, the channel bed and formerly active bars are largely static, and riparian vegetation has encroached into the formerly active channel.

In addition to the effects of flow regulation and loss of sediment supply from the upper watershed, this reach has been extensively modified by gold

dredging. Gold mining in the DTR began approximately a century ago and continued through the 1950s. As part of the gold mining, channel and floodplain sediment deposits were excavated to bedrock and then re-deposited in rows covering approximately 7.6 square miles of floodplain (Figure 1). These tailings consist of fine sand and gravel overlain by cobbles and boulders (Goldman 1964), a stratification pattern that resulted from the sluicing and discharge process. As a result of gold dredging, the channel has been depleted of coarse sediment and the adjacent floodplain has been raised and covered with dredger tailings piles. An estimated 24 million cubic yards of dredger tailings currently cover approximately 7.6 square miles of the floodplain in this reach and in the dredged area upstream of Crocker-Huffman Dam (Stillwater Sciences 2001). An improved estimate of the total volume of dredger tailings within the DTR will be calculated in a later phase of this project.

The combined effects of gold dredging, flow regulation, elimination of coarse sediment supply, and land use development have converted this reach from a complex, multiple-channel system to a simplified, single-thread system with a narrow floodplain. The complex slough channels that once dominated the floodplain have been converted to agricultural irrigation and return-flow ditches. The dredger tailings on the floodplain constrain the river channel so that high flow events are prevented from spilling onto the floodplain. As such, although high flow events are now rare, even moderate flow events are capable of resulting in high shear stresses that are highly effective at transporting finer sediment. Over time, the occasional high flow events combined with the lack of sediment supply have acted to transport the majority of finer sediments from the reach. One result of this high finer sediment transport capacity is the very coarse bed surface of the reach, which is composed of coarse gravel and cobble. The D_{50} (the median particle size) of the bed surface ranges from 28 to 134 mm, and the D_{84} (value for which 84% of the particles are finer) ranges from 68 to 270 mm (CDWR 1994, Vick 1995, Stillwater Sciences 2001 and 2004). Another result has been that the channel is now typified by long, deep pools that are scoured to bedrock or to a coarse cobble armor layer. These pools are partly controlled by bedrock outcrops and some of them are quite likely the result of dredger mining in the channel. The pools are separated by riffles that are also partly controlled by bedrock, but many of which are also maintained through frequent gravel augmentation of spawning riffles and water diversion wing-dams. The channel slope averages 0.0023 (Stillwater Sciences 2004).

The primary restoration issues in the DTR include flow reduction and alteration of seasonal flow patterns, a channel bed that is too coarse to

accommodate salmonids spawning, lack of bed-mobilizing flows, lack of coarse sediment supply, and conversion of the floodplain to tailings piles.

Removal of the tailings from the floodplain will yield multiple restoration opportunities and ecosystem benefits, including:

- providing area for riparian vegetation to establish;
- allowing the channel to be re-shaped to promote bed mobility; and
- allowing the floodplain to be graded to encourage more frequent inundation.

1.2 Project Overview and Objectives

The sediment transport model reported in this technical memorandum was developed as a part of the Merced River Corridor Restoration Plan Phase IV: Dredger Tailings Reach project (California Bay-Delta Authority [CBDA] ERP-02-P12-D), which will evaluate strategies for channel and floodplain restoration of the 318-acre Merced River Ranch and, by implication, for the 7-mile DTR.

The DTR has become a focus for restoration planning for several reasons. First, the DTR is now the primary spawning area in the Merced River for fall Chinook salmon (*Oncorhynchus tshawytscha*), an important management species and a candidate for listing under the federal Endangered Species Act, and, potentially, steelhead (*O. mykiss*) (Stillwater Sciences 2002), which is listed as threatened under the federal Endangered Species Act. Salmonid species that historically migrated up the Merced River now concentrate spawning in the DTR directly downstream of Crocker-Huffman Dam, the current upstream limit of salmonid migration. Lastly, past and current studies and restoration planning in the Merced River have provided a cursory understanding of the physical and ecological conditions of the reach and factors limiting ecosystem health. These studies include the Anadromous Fish Restoration Program's (AFRP) Comprehensive Assessment and Management Program; U.S. Geological Survey and Central Valley Regional Water Quality Control Board water quality monitoring; Merced Irrigation District (Merced ID) and the California Department of Fish and Game (CDFG) salmon population ecology studies; and Stillwater Sciences' AFRP and CBDA-funded geomorphic and riparian vegetation evaluations.

Partly in response to these studies, the CBDA Ecosystem Restoration Program funded the development of the Merced River Corridor Restoration Plan (Stillwater Sciences 2002). The restoration planning process was designed to provide a technically sound, publicly supported, and

implementable plan to improve geomorphic and ecological functions in the Merced River corridor from Crocker-Huffman Dam to the confluence with the San Joaquin River. The Restoration Plan identifies restoration objectives and provides recommendations for the Merced River based on current scientific understanding of the river with input from the Merced River Stakeholders (MRS), Technical Advisory Committee (TAC), and the broader public. Since the restoration objectives were discussed by a broad spectrum of interests represented by the MRS, TAC, and public, they address not only geomorphic and ecological restoration in the river but also the concerns of local citizens, landowners, and other stakeholders. In the DTR, which is affected by flow reduction and alteration of seasonal flow patterns, lack of bed-mobilizing flows, lack of coarse sediment supply, conversion of the floodplain to tailings piles, and channel confinement, the following reach-scale restoration objectives were recognized:

- Balance sediment supply and transport capacity to allow the accumulation and retention of spawning gravel and prevent riparian vegetation encroachment;
- Restore floodplain functions to improve the establishment of riparian vegetation and the quality of riparian habitat;
- Increase in-channel habitat complexity to improve aquatic habitat for native aquatic species; and
- Scale low-flow and bankfull channel geometry to current flow conditions.

The Merced River Corridor Restoration Plan Phase IV: Dredger Tailings Reach project begins to address the restoration objectives for the DTR developed in the Restoration Plan. The goals of the DTR project are to design pilot experiments in the channel and floodplain to test measures that will initiate the restoration of natural ecosystem function in the reach to the extent feasible. The current project is the precursor for conducting experimental pilot projects in floodplain and channel restoration, gravel augmentation, and floodplain re-vegetation. Removal of the tailings from the floodplain has the potential to yield multiple restoration opportunities and ecosystem benefits, but the actual detailed impact of such activities is largely unknown. The experiments designed as part of this project will increase the collective scientific understanding of the potential for dredger tailings removal and re-use (e.g., as material to fill the channel), and is intended to improve restoration effectiveness and reduce project uncertainty when implementing similar schemes in the future. Future projects will be implemented to increase coarse sediment storage in the Merced River channel, balance bed texture with sediment transport competence, remove dredger tailings to create diverse floodplain surfaces at functional elevations, and reconstruct a channel through a portion of the DTR.

A comprehensive understanding of the sediment transport dynamics in which the river currently functions is required to address the reach-scale restoration objectives described in the Restoration Plan and meet the goals of the DTR project. For this reason, a reach-scale sediment transport model was developed as a part of the DTR project. The objectives of the sediment transport model are:

- Predict sediment transport rates, spatial and temporal coarse sediment deposition patterns, and bed surface and bedload grain-size.
- Refine the estimate of the volume and texture of sediment needed for the initial infusion and long-term augmentation.
- Predict sediment routing through the reach to ensure sediment placed in the reach as part of restoration activities can route downstream.

Augmented gravel is often introduced as pulses into the river channel, which must be accounted for in sediment transport models that attempt to simulate restored conditions. We have used models presented in Cui and Parker (in press) to assess sediment pulses in several channels. The Cui and Parker (in press) model was developed for gravel-bedded alluvial rivers to examine the evolution of gravel pulses. It can predict the evolution of the channel bed, including the thickness of sediment deposits and grain size characteristics. Application of the Cui and Parker (in press) model to simulate the evolution of a natural landslide in the Navarro River, CA produced results very similar to field measurements (Hansler 1999, Lisle et al. 2001, Sutherland et al. 2002). Simulation of a set of laboratory experiments appropriate for model validation with a simplified version of Cui and Parker (in press) also produced good results (Cui and Parker in press, Cui et al. 2003a,b).

The Cui and Parker (in press) model has also been adapted to simulate sediment transport following the removal of dams (e.g., Cui and Wilcox in press, Cui et al. in press [a,b]), where the release of the reservoir sediment deposit represents the initial sediment pulse. Despite the many models derived using variations of Cui and Parker (in press), the model must be further adapted for this project to accommodate site-specific issues that may be more important to accurately simulate potential restoration strategies on the Merced River. In particular, the adapted model must include floodplains, which may be re-graded to increase the frequency of floodplain inundation. The inclusion of floodplains will reduce the sediment transport capacity during overbank flow events and, thus, may influence the amount of gravel required for augmentation. The adaptation of the model is discussed below in Section 2.

The results of the simulation for existing conditions are reported in this technical memorandum.

2 GOVERNING EQUATIONS AND SOLUTION TECHNIQUE

As discussed earlier, in order to accurately model sediment transport in the DTR, the floodplains must to be included in the Merced River DTR Sediment Transport Model. For simplicity, cross-sections used in the model are separated into three components: a main channel and two floodplains, and each component is further simplified as a rectangle, rather than the complex topography often seen in river channels (Figure 2).

The governing equations for resistance and flow are adapted from Cui and Parker (in press) with modifications to include the floodplains, which include: continuity for water flow, equation (1); Manning-Strickler resistance equation in the main channel, equation (2); Manning's equation on floodplains, equations (3a,b); relations for water depths on the floodplains and the main channel, equations (4a,b); the relation between roughness and surface grain size distribution by Cui et al. (1996), equation (5); the momentum equation for steady flow, equation (6); and a channel geometric relation, equation (7).

$$Q_w = Q_c + Q_{fl} + Q_{fr} \quad (1)$$

$$\frac{Q_c}{B_c h_c \sqrt{g h_c S_f}} = 8.1 \left(\frac{h_c}{k_s} \right)^{1/6} \quad (2)$$

$$Q_{fl} = \frac{1}{n_{fl}} B_{fl} h_{fl}^{5/3} S_f^{1/2}, \quad Q_{fr} = \frac{1}{n_{fr}} B_{fr} h_{fr}^{5/3} S_f^{1/2} \quad (3a,b)$$

$$h_{fl} = \max(0, h_c + \eta + \eta_b - \eta_{fl}), \quad h_{fr} = \max(0, h_c + \eta + \eta_b - \eta_{fr}) \quad (4a,b)$$

$$k_s = 2D_{sg} \sigma_{sg}^{1.28} \quad (5)$$

$$\frac{d}{dx} \left(\frac{Q_w^2}{2A^2} + g(\eta_b + \eta + h_c) \right) + gS_f = 0 \quad (6)$$

$$A = B_c h_c + B_{fl} h_{fl} + B_{fr} h_{fr} \quad (7)$$

Many of the variables in equations (1) through (7) are shown graphically in Figure 2, and all of them are listed below, in alphabetical order: A denotes flow area, including the main channel and the floodplains; B_c denotes the width of the main channel; B_{fl} and B_{fr} denote the width of the left and right floodplains, respectively; D_{sg} denotes surface particle geometric mean grain size; g denotes acceleration of gravity; h_c denotes water depth in the main channel; h_{fl} and h_{fr} denote water depth over left and right floodplains, respectively; k_s denotes roughness height; n_{fl} and n_{fr} denote Manning's n value on the left and right floodplains, respectively; Q_c denotes water discharge in the main channel; Q_{fl} and Q_{fr} denote water discharge on the left and right floodplains, respectively; Q_w denotes total water discharge; S_f denotes friction slope; x denotes downstream distance; η denotes the thickness of sediment deposit in the main channel; η_b denotes a base elevation over which the sediment deposition thickness is measured; η_{fl} and η_{fr} denote the elevations of the left and right floodplains, respectively; and σ_{sg} denotes the geometric standard deviation of the surface sediment particles.

Combining equations (1), (2), and (3a,b) results in the following equation for friction:

$$S_f = \left[\frac{Q_w}{8.1B_c \left(\frac{1}{k_s} \right)^{1/6} \sqrt{gh_c}^{5/3} + \frac{1}{n_{fl}} B_{fl} h_{fl}^{5/3} + \frac{1}{n_{fr}} B_{fr} h_{fr}^{5/3}} \right]^2 \quad (8)$$

and equation (6) can be rewritten into the following standard backwater equation:

$$\frac{dh_c}{dx} = \frac{S_0 - S_f}{1 - Fr^2} \quad (9)$$

in which Fr denotes the local Froude number defined as

$$F_r = \frac{Q_w}{\sqrt{gA^3/B}} \quad (10)$$

where B is the width of water surface (main channel and floodplains combined, if inundated).

Flow parameters are solved with the backwater equation, equation (9), when the Froude number is smaller than 0.8.

When the Froude number F_r is greater than 0.8, the quasi-normal flow assumption is applied instead of the standard backwater equation, i.e.,

$$S_f = S_0 = -\frac{\partial(\eta_b + \eta)}{\partial x} \quad (11)$$

in which S_0 denotes bed slope. A combination of equations (8), (11), and (4a,b) will allow for the solution of water depths in the main channel and over floodplains. Cui et al. (in press [a]) demonstrated that the above simplified solutions for flow, i.e., solving the backwater equation under low Froude number conditions and applying quasi-normal flow assumptions under high Froude number conditions, produced excellent results for sediment transport simulations.

Since the transport of sediment is computed on a grain size-specific basis, it is first necessary to specify how the grain size distribution of gravel is discretized before the sediment transport and continuity equations are introduced. Here the relevant sediment is only the bedload coarser than 2 mm. Grain size D can be equivalently characterized in terms of the (base-2) logarithmic ψ -scale;

$$\psi = -\phi = \log_2(D) \quad (12)$$

In the above relation ϕ denotes the ϕ -scale familiar to sedimentologists. Use is made of the ψ -scale instead of the ϕ -scale because it is more intuitive, with an increase in grain size corresponding to an increase in the ψ -scale. Gravel grain size distributions are discretized into N bins $j = 1, 2, \dots, \text{and } N$, bounded by $N + 1$ grain sizes $D_1 \dots D_{N+1}$ ($\psi_1 \dots \psi_{N+1}$) progressing from smaller to larger size as j increases. Here D_1 always corresponds to 2 mm (i.e. a value of ψ_1 of 1), i.e., the boundary between sand and gravel. The j -th grain size range is bounded by the sizes D_j and D_{j+1} , and has the characteristic size

$$\bar{D}_j = \sqrt{D_j D_{j+1}}, \quad \bar{\psi}_j = \log_2(\bar{D}_j) = \frac{1}{2}(\bar{\psi}_j + \bar{\psi}_{j+1}) \quad (13a,b)$$

The fractions of gravel of the j -th grain size range in the surface layer of the stream and the bedload are denoted respectively as F_j , and p_j , where both are normalized to sum to unity over all gravel sizes. The formulation presented below also uses surface fractions F_j' that have been adjusted according to Parker (1991a,b) to reflect exposed surface area available for abrasion;

$$F_j' = \frac{F_j / \sqrt{D_j}}{\sum F_j / \sqrt{D_j}} \quad (14)$$

It is assumed that sediment transport occurs only within the main channel, while the floodplains may serve as flood ways (i.e., water may be conveyed over the floodplains, but bedload transport will not occur on them). This assumption is appropriate because sediment deposition on floodplains is almost always from the suspended load and finer than 2 mm, which is not considered in this analysis. The Exner equations of sediment continuity, given below in equations (15) and (16), are simplified from those in Cui and Parker (in press) in that only one lithology (rock type) is allowed, i.e., all the sediment particles are assumed to have the same abrasion coefficient, i.e.:

$$(1 - \lambda_p) B_c \frac{\partial \eta}{\partial t} + \frac{\partial Q_s}{\partial x} + \beta Q_s \left(2 + \frac{1}{3 \ln(2)} \frac{p_1 + F_1'}{\psi_2 - \psi_1} \right) = 0 \quad (15)$$

$$(1 - \lambda_p) B_c \left(\frac{\partial(L_a F_j)}{\partial t} + \frac{(\eta - L_a)}{\partial t} \right) + \frac{\partial(Q_s p_j)}{\partial x} + \beta Q_s (p_j + F_j') + \frac{\beta Q_s}{3 \ln(2)} \left(\frac{p_j + F_j'}{\psi_{j+1} - \psi_j} - \frac{p_{j+1} + F_{j+1}'}{\psi_{j+2} - \psi_{j+1}} \right) = 0 \quad (16)$$

in which λ_p denotes porosity of the sediment deposit; t denotes time; Q_s denotes volumetric transport rate of sediment; β denotes volumetric abrasion coefficient (i.e., fraction of volume lost over a unit distance for gravel particles); L_a denotes surface layer thickness; p_1 and F_1' are p and F' values for the finest size group, respectively; and ψ_1 and ψ_2 are the finer and coarser bounds for the finest size group.

The sediment transport equation used to evaluate sediment transport capacity in the model is the surface-based bedload equation of Parker (1990), which calculates sediment transport capacity and the associated grain size

distribution based on local shear stress and surface grain size distribution. Details of the surface-based bedload equation of Parker (1990) can be found in the original reference and is not discussed here. Of interest for this report is the parameter ϕ_{sgo} , which is the surface geometric-mean-based Shields stress (τ_{sgo}^*) normalized with a reference Shields stress (τ_{rsgo}^*) with a value of 0.0386:

$$\phi_{sgo} = \frac{\tau_{sgo}^*}{\tau_{rsgo}^*}, \quad \tau_{sgo}^* = \frac{h_c S_f}{RD_{sg}}, \quad \tau_{rsgo}^* = 0.0386 \quad (17a,b,c)$$

in which R denotes the submerged specific weight of sediment particles; and D_{sg} denotes the geometric mean grain size of the surface layer sediment. Parker's (1990) surface-based bedload equation does not contain a critical Shields stress, which is defined as the Shields stress at which bed mobility begins. The reference Shields stress, however, can be viewed as a surrogate for critical Shields stress. The surface-based equation of Parker (1990) is designed so that sediment transport capacity will decrease quickly to almost zero when the local Shields stress becomes less than reference Shields stress (i.e., parameter ϕ_{sgo} becomes less than unity). With that, ϕ_{sgo} is used to gauge channel bed mobility and to consider $\phi_{sgo} = 1$ as the threshold for channel bed mobility in the subsequent simulations, as discussed later in Section 4.

3 INPUT PARAMETERS

The following boundary conditions are applied for the simulation:

1. discharge in the simulation reach over the period of simulation;
2. set bed elevation and normal flow assumption at the downstream end;
and
3. sediment supply (natural and artificial) rate and associated grain size distribution at the upstream end.

In addition, user-defined gravel augmentation can be assessed by introducing gravel pulses of specified amount and grain size distribution at different locations. This feature is important because periodic gravel augmentation has occurred within the DTR and is expected to continue as an integral restoration strategy in the future.

3.1 Hydrology

Daily average discharge at the Merced River below Merced Falls Gauge (USGS # 11270900) for the post New Exchequer Dam period between 10/1/1972 and 9/30/2002 (water years 1973 – 2002) was used for the simulation (Figure 3). There are a few small water diversions but no tributaries within the DTR. Some of the water diversions are shown as wing dams in Figures 1 and 4. The volume of water diverted, however, is relatively small during high flow events when the majority of sediment transport occurs, and thus is ignored in the simulation. As a result, the model assumes that discharge does not vary spatially throughout the DTR.

3.2 Longitudinal Profile and Cross-sections

The Merced River DTR has a length of approximately 11 km (6.8 miles). Stillwater Sciences (2004) surveyed 40 cross-sections within the main channel area, the locations of which are shown in Figures 1 and 4. Those cross-sections were further extended to include the floodplains, terraces, or dredger tailings piles on the two banks using photogrammetry conducted by KSN, Inc. (Stillwater Sciences 2004). In addition, KSN, Inc. also surveyed

thalweg elevation throughout the reach (Stillwater Sciences 2004). In order to proceed with the sediment transport modeling exercise, the available cross-sections were further processed so that the main channel and the two floodplains, terraces, or dredger tailings piles (all of which will be referred to as floodplain hereafter) can be simplified as rectangles, as shown in the sketch in Figure 2, and as an example in Figure 5. The parameters of the simplified cross-sections were then interpolated to longitudinal stations located approximately 110 m (360 ft) apart, based on values from the nearest survey locations, including main channel width (B_c), left and right floodplain widths (B_{fl} and B_{fr}), and the elevation differences between the floodplains and the main channel bed ($\eta_{fl} - \eta - \eta_b$ and $\eta_{fr} - \eta - \eta_b$). The 110-m spacing corresponds to approximately 2 to 2.5 times the average bankfull channel width in the reach, which is consistent with the general resolution of one-dimensional sediment transport modeling. During the interpolation process, a small amount of random variation was added to each of the geometric parameters so that the interpolated parameters can be offset a random amount from the linearly interpolated values to represent the local variability common to natural rivers. The maximum allowable offsets from the linearly interpolated values for the main channel width, floodplain widths, and elevation differences between floodplains and the main channel bed were 10 m (30 ft), 30 m (90 ft), and 0.7 m (2.3 ft), respectively. The bed elevations at the stations are interpolated from the thalweg elevation surveyed by KSN, Inc. and presented in Stillwater Sciences (2004). The bed elevations of the main channel from cross-sectional and thalweg surveys, and the interpolated values are shown in Figure 4. It should be noted that the interpolated main channel bed elevations shown in Figure 4 are used as the initial profile for the simulation with an assumption that the thickness of the sediment deposit is 0.5 m (1.6 ft) (i.e., the base elevation is 0.5 m [1.6 ft] lower than shown in Figure 4). The thickness of sediment deposit will be allowed to evolve in a “zero process”, described in Section 4, so that the background condition will actually be generated with the numerical model.

3.3 Surface Grain Size Distributions

Surface grain size distributions are interpolated based on 24 pebble counts collected by Stillwater Sciences (2004) during the summer of 2003, as shown in Figure 6. Locations of the pebble counts are shown in Figure 1. More details about surface texture of the study reach, e.g., more accurate locations of the pebble counts and facies mapping of the reach, can be found in Stillwater Sciences (2004). There are significant variations in characteristic grain sizes along the river within the study reach, as shown in Figure 7. The median grain size (D_{50}) of Stillwater Sciences (2004) pebble counts, for

example, ranges between a maximum value of 133 mm and a minimum value of 42 mm. In particular, the characteristic grain sizes a short distance downstream of Crocker-Huffman Dam are finer than most of the reach, most likely as a result of the gravel augmentation by California Department of Water Resources (CDWR) and CDFG. The finer characteristic grain sizes are also observed at the locations of three wing dams at approximately 6.9 km (4.3 mile), 9.3 (5.8 mile), and 11.2 km (7.0 mile) downstream from Crocker-Huffman Dam (Figure 7).

3.4 Coarse Sediment Supply

The Merced River DTR currently receives very little coarse grained sediment because New Exchequer Dam intercepts all the coarse sediment supply from the steeper upper watershed. Downstream of New Exchequer Dam, the contributing watershed is flatter and coarse sediment supply is limited. In addition, it is very likely that several small diversion dams upstream of the DTR, such as Crocker-Huffman Dam, intercept the majority of the limited coarse sediment supply that originates between New Exchequer Dam and the DTR. Despite the many dams upstream, it is reasonable to assume that a small amount of bedload may reach the DTR, either by escaping from the upstream reservoirs formed by small diversion dams, or by limited bank erosion during extremely high flow events. The frequency and volume of coarse sediment supply to the DTR is unknown. CDWR and CDFG have been augmenting gravel in the upstream portion of the DTR since 1991, and the amount of gravel augmented during the past 14 years (discussed in detail in Section 3.5) is likely far more than the amount of natural gravel supply from either upstream reaches or bank erosion. In addition, three diversion wing dams were constructed with gravel (Figure 8), which also introduce sediment to the river. Overall, it is reasonable to believe that the amount of natural sediment supply is so small that its exact value will not have significant effect on the results of the simulation. Here, for simplicity, the long-term average natural sediment loading to the DTR is assumed to be 0.2 metric tons (0.22 tons) per year, which is used to establish the background condition of the numerical model in a zero process, as discussed below. It needs to be stressed that the 0.2 metric tons (0.22 tons) of long-term average annual sediment supply is not based on field data, nor is it based on any analysis. The exact value for long-term sediment supply is not important to the simulation, as long as the sediment supply to the DTR is low. This has been confirmed in a sensitivity test in which the sediment supply was increased by a factor of 100, i.e., to 20 metric tons (22 tons) per year. The natural sediment supply is distributed in time according to

discharge, the details of which are not important to this project due to the minimal natural sediment supply, and are not discussed here.

3.5 Gravel Augmentation and Wing Dams

There have been two gravel augmentation projects within the study reach: one maintained jointly by CDWR and CDFG since 1991 at the Merced River Hatchery (Kevin Faulkenberry, pers. comm.), and the other by CDFG in 2003 at Maury's Riffle immediately downstream of Crocker-Huffman Dam (Doug Ridgeway, pers. comm.). The locations of both gravel augmentation projects are within 0.1 km (300 ft) downstream of Crocker-Huffman Dam (Figure 4). The estimated amount of gravel augmentation at the Merced River Hatchery and Maury's Riffle since the inception of the projects are given below in Table 3-1. Kevin Faulkenberry (pers. comm.) provided the estimated grain size distribution for the augmented gravel at the Merced River Hatchery site, as shown in Figure 9. Grain size distribution for the Maury's Riffle gravel augmentation is not available but it is expected to be similar to values provided in Figure 9 for the year 2003 since it is likely that the sediment used in the two augmentations came from the same source.

Table 3-1. Amount of gravel augmentation at the upstream end area of the Dredger Tailings Reach.

Year	Amount of gravel augmentation (metric tons)*	Augmentation locations
1991	2,600	Merced River Hatchery
1996	930	Merced River Hatchery
1997	910	Merced River Hatchery
2000	1,030	Merced River Hatchery
2003	2,450	Merced River Hatchery (1,360 metric tons) and Maury's Riffle (1,090 metric tons)

* 1 metric ton = 1.1 ton

Several water diversion wing dams downstream of Crocker-Huffman Dam have utilized spawning-sized gravel for construction in recent years. Among them, wing dams #3, #4, and #5 are located within the DTR, as shown in Figures 1, 4, 7, and 8. Wing dam #5 is located at the downstream end of the DTR, and thus, its presence will not have a significant effect on bed texture in the study reach. For this reason, wing dam #5 will not be included in this study. CDFG provided gravel for the construction of these wing dams in 2000 and again in 2002. The amount of gravel provided by CDFG for the initial construction of gravel wing dams #3 and #4 in 2000 is unknown, but approximately 630–720 metric tons were provided to reconstruct each wing

dam in 2002 (Doug Ridgeway, pers. comm.). For the purpose of the simulation presented in Section 5, it is assumed that 675 metric tons of gravel was introduced to each of wing dams #3 and #4 in 2000. The specific grain size distribution of the gravel is unknown but is expected to be similar to that shown in Figure 9.

In the model, gravel augmentations and wing dams are introduced as sediment pulses of specified grain size distributions at specific locations. The augmented gravel volume is assumed to be uniformly distributed across the channel and within the nodes of the augmentation area, which tapers linearly to zero thickness at the upstream end and downstream end nodes of the augmentation area, as shown in Figure 10. It should be noted, however, that the grid spacing used in this simulation exceeds the dimensions of individual wing dams, and thus the detailed impacts of individual dams cannot be accurately represented by the model. The introduced amounts of gravel at the wing dam sites, however, faithfully represent the amounts introduced in the field, and thus, the sediment transport characteristics beyond the localities of the wing dams should be accurate.

4 ZERO PROCESS AND SIMULATION OF BACKGROUND CONDITIONS PRIOR TO GRAVEL AUGMENTATION

One of the necessary steps in sediment transport simulation is a zero process (e.g., Cui and Wilcox, in press), which simulates the river under the assumed background conditions for a long period of time. The zero process can be viewed as the natural process with which the river adjusts itself in time to produce the current geomorphic conditions. During the zero process, certain parameters may be adjusted so that the model performs more reasonably when compared to field data or field observations. The zero process was designed to allow only natural sediment supply. The gravel augmented by CDWR and CDFG and the gravel from construction of wing dams will be introduced later in Section 5 when the current conditions are evaluated. The results of the zero process will be used as the initial condition for the subsequent numerical runs (i.e., during simulation of future restored conditions).

During the zero process, the thickness of sediment deposit was initially set to 0.5 m (1.6 ft), as discussed earlier in Section 3.2, and the model was run repeatedly until a quasi-equilibrium condition was established. Under this quasi-equilibrium condition, the channel bed does not degrade or aggrade on a long-term average basis, although it may aggrade or degrade on a year-to-year basis. Once the quasi-equilibrium condition was realized, the background condition was evaluated by running the model for 30 more years, with the same input data as the zero process.

A 30-year simulation (Figure 3) under the assumed background conditions indicates a low degree of existing sediment transport and floodplain inundation, and very little change in channel bed elevation and surface texture between years (Figure 11 and Figure 12). Simulation results further show that the modeled flow cannot access the adjacent terraces and dredger tailings piles except at one location, approximately 11 km (6.8 mile) downstream from Crocker-Huffman Dam, where the flow reached the left bank four times during a 30-year period. It should be noted, however, that

although the sediment transport model is not intended to accurately simulate the water surface profile, the modeled low frequency of overbank flow is considered realistic. More accurate water surface simulation was achieved with a recently developed HEC-RAS model of the DTR (see URS Corporation 2004 for detail). Despite the limitations of the sediment transport model in accurately simulating the water surface profile, the low frequency of over bank flow should be noted.

In order to assess modeled sediment transport within the DTR for the zero process simulation, bed mobility was defined according to the simulated normalized Shields stress ϕ_{sgo} , as shown in Table 4-1 below. Normalized Shields stress can range from less than 1 (immobile bed surface) to greater than 1.6 (very mobile bed surface). The current classification of bed mobility for the zero process is preliminary and may be adjusted in the future when more data are available, either from this project or from field observations elsewhere.

Table 4-1. An arbitrary definition of channel bed mobility according to the normalized Shields stress ϕ_{sgo} in the surface-based bedload equation of Parker (1990), where the description of each bed mobility stage is rather speculative.

Definition	Description
$\phi_{sgo} < 1.0$	Non-mobile channel bed – particles on channel bed are not expected to move.
$1.0 \leq \phi_{sgo} < 1.3$	Marginally mobile channel bed – individual particles on channel bed may be entrained by the flow, although tracer particles are unlikely able to detect such bed mobility.
$1.3 \leq \phi_{sgo} < 1.6$	Moderately mobile channel bed – bed mobility is likely detectable with tracer particles.
$\phi_{sgo} \geq 1.6$	Functionally mobile channel bed – bed mobility is detectable by tracer particles; bed mobility may achieve certain desired ecological functions.

Zero process simulation results indicate that the flow cannot mobilize the channel bed within the DTR during most years modeled. For wet years with relatively high flow events, bed mobility occurs only at a few locations. To demonstrate the spatial distribution of channel bed mobility for a wet year, simulation results for water year 1983, which was an extremely wet year (see Figure 13 and Figure 14), are presented in Figure 15. Comparisons of bed mobility with river longitudinal profile (Figure 15a) and surface median grain size (Figure 15b) indicate that the locations with relatively high bed mobility are located at places with relatively high gradient and generally with relatively small surface grain size. For water year 1983 in particular, all the locations where modeled sediment transport occurred have surface

median grain sizes less than 60 mm. The high degree of modeled bed mobility at two locations in particular, approximately 7 km (4.3 mile) and 9.5 km (5.9 mile) downstream of Crocker-Huffman Dam, is most likely the result of the wing dams at those locations (i.e., steep thalweg profile and relatively small bed particles). In general, model results indicate that, under the post New Exchequer Dam hydrologic conditions, the Merced River DTR lacks channel mobility that is beneficial to certain natural ecological functions.

5 EVALUATION OF CURRENT CONDITIONS

Following the zero process simulation, the current sediment transport conditions within the DTR were evaluated by including the past gravel augmentation projects and construction of wing dams discussed in Section 3.5 in the simulation.

Model simulation indicates that gravel augmentation has resulted in localized changes in bed elevation and surface texture at the augmentation site, as shown in Figures 16, 17 and 18, relative to background conditions discussed in Section 4. At approximately 250 m (820 ft) downstream of Crocker-Huffman Dam, the CDWR/CDFG gravel augmentation had resulted in approximately 2.5 cm (1 inch) of aggradation and a decrease in median grain size from 55 mm to 49 mm. At approximately 0.5 km (0.3 mile) downstream of Crocker-Huffman Dam and beyond, neither bed elevation nor surface grain size have changed as the result of the CDWR/CDFG gravel augmentation. It should be noted that the lack of significant decrease in median grain size at gravel augmentation sites is most likely the result of having to use the post-gravel augmentation grain size distributions and channel geometry to simulate background conditions because pre-gravel augmentation grain size distribution and channel geometry data were not available. That is, gravel augmentation may have resulted in much more significant decrease in local particle grain size than indicated in the model run because the initial condition used in the model run does not really reflect the true pre-gravel augmentation condition.

Overall, the simulation results suggest that gravel augmentation and wing dam construction at the current intensity will have localized effects in aggrading the channel bed and decreasing surface grain size, but may not have reach-scale effects because the river does not have the energy to transport a significant amount of bedload. It should be noted that local spatial adjustment (e.g., within the scale of the calculation grid) of gravel pulses cannot be simulated because it is beyond the resolution of a numerical model. Field observations and measurements coincide with the model simulation results in that documented sediment transport at gravel augmentation and wing dams is localized. For a frequently occurring high flow of approximately 40 m³/s (1,400 cfs), surface sediment at the gravel

augmentation riffle adjacent to the Merced River Hatchery has been shown to move up to 7 m (20 ft) (Akagi 1994) and surface bed particles at wing dam #5 has been shown to move up to 40 m (130 ft) (MID 2003). Similarly, recent field experiments conducted by Stillwater Sciences (unpublished data) on the DTR show maximum coarse sediment (D_{84}) movement of approximately 7.3 m (24 ft) at the Merced River Hatchery augmentation riffle, and a maximum coarse sediment movement of approximately 18.3 m (60 ft) at wing dam #5 for a peak flow of approximately 53 m³/s (1,870 cfs).

6 CONCLUSIONS AND DISCUSSION

A bedload transport model was constructed for the Merced River DTR based on the sediment pulse model of Cui and Parker (in press). The current model allows for inclusion of floodplains (or terraces and dredger tailings piles) on both banks to serve as floodways when inundated. The model also allows for the inclusion of gravel augmentation and construction of gravel wing dams as gravel pulses.

Simulation of the background condition, where no gravel is introduced to the river artificially, suggests that daily mean flows over the last 30 years have been largely incapable of inundating the floodplain (see also URS 2004) and have not had the required energy to mobilize the existing channel bed except in a few locations during extremely high flow events. Simulation of the current condition, where gravel is introduced from augmentation sites and by construction of wing dams, and observation of grain size patterns in the DTR indicate that the introduced gravel has some localized effect in aggrading the channel bed and decreasing surface median grain size. Model results suggest that the ongoing gravel augmentation and wing dam construction have not resulted in reach-scale effects on the study reach although, locally, both aggradation and a decrease in median grain size are clearly visible.

This model will be used as the basis for simulating the likely sediment transport impacts of DTR restoration strategies planned in future stages of this project.

Acknowledgements: The useful comments of peer reviewers, Kevin Faulkenberry, Kris Vyverberg, and Peter Wilcock, have been incorporated into this document.

7 REFERENCES

Akagi, Y. 1994. Sediment transport at sites of spawning gravel enhancement on the Merced River below the Crocker-Huffman Dam. Masters Thesis, Department of Civil Engineering, University of California, Berkeley.

CDWR (California Department of Water Resources). 1994. San Joaquin River tributaries spawning gravel assessment: Stanislaus, Tuolumne, and Merced Rivers. Memorandum Report. CDWR, Northern District.

Cui, Y., Parker, G., and Paola, C. 1996. Numerical simulation of aggradation and downstream fining. *Journal of Hydraulic Research*, 34(2), 185-204.

Cui, Y., Parker, G., Lisle, T., Gott, J., Hansler, M., Pizzuto, J.E., Allmendinger, N.E., and Reed, J., G. 2003a. Sediment pulses in mountain rivers. Part I: experiments. *Water Resources Research*, 39(9), 1239, doi: 10.1029/2002WR001803.

Cui, Y., Parker, G., Pizzuto, J., and Lisle, T. 2003b. Sediment pulses in mountain rivers. Part II: comparison between experiments and numerical predictions. *Water Resources Research*, 39(9), 1240, doi: 10.1029/2002WR001805.

Cui, Y., and Parker, G. (in press). Numerical model of sediment pulses and sediment supply disturbances in mountain rivers. *Journal of Hydraulic Engineering*, HY/2002/023176.

Cui, Y. and Wilcox, A. (in press). Development and Application of Numerical Modeling of Sediment Transport Associated with Dam Removal. in Garcia, M.H., ed., *Sedimentation Engineering*, ASCE Manual 54 (II).

Cui, Y., Parker, G., Braudrick, C., Dietrich, W.E., and Cluer, B. (in press, a). Dam Removal Express Assessment Models (DREAM). Part 1: Model development and validation. *Journal of Hydraulic Research*.

Cui, Y., Braudrick, C., Dietrich, W.E., Cluer, and Parker, G., B. (in press, b). Dam Removal Express Assessment Models (DREAM). Part 2: Sample runs/sensitivity tests. *Journal of Hydraulic Research*.

Goldman, H.B. 1964. Sand and gravel in California: an inventory of deposits. Part B – Central California. Bulletin No. 180-B. California Department of Mines and Geology, Sacramento, California.

Hansler, M.E. 1999. Sediment wave evolution and analysis of a one-dimensional sediment routing model, Navarro River, Northwestern California. M.S. Thesis, Humboldt State University, December, 128p.

Lisle, T.E., Cui, Y., Parker, G., Pizzuto, J.E., and Dodd, A.M. 2001. The dominance of dispersion in the evolution of bed material waves in gravel-bed rivers. *Earth Surface Processes and Landforms*, 26, 1409-1420.

MID (Merced Irrigation District). 2003. Merced River wind dam gravel monitoring 2000-2002, Final Report. Conducted with Natural Resources Scientists, Inc. for the U.S. Fish and Wildlife Service Anadromous Fish Restoration Program.

Parker, G. 1990. Surface-based bedload transport relation for gravel rivers, *Journal of Hydraulic Research*, 28(4), 417-436.

Parker, G. 1991a. Selective sorting and abrasion of river gravel. I: Theory. *J. Hydr. Engrg.*, 117(2), 131-149.

Parker, G. 1991b. Selective sorting and abrasion of river gravel. II: Application. *J. Hydr. Engrg.*, 117(2), 150-171.

Stillwater Sciences. 2001. Merced River Corridor Restoration Plan Baseline Studies Volume II: Geomorphic and riparian vegetation investigations. Prepared by Stillwater Sciences, Berkeley, California for CALFED, Sacramento, California.

Stillwater Science. 2002. Merced River Corridor Restoration Plan. Prepared by Stillwater Sciences, Berkeley, California, for CALFED, Sacramento, California.

Stillwater Sciences. 2004. Channel and floodplain surveys of the Merced River Dredger Tailings Reach. Stillwater Sciences, Berkeley, CA.

Sutherland, D.G., Hansler, M.E., Hilton, S., and Lisle, T.E. 2002. Evolution of a landslide-induced sediment wave in the Navarro River, California. *Geological Society of America Bulletin*, 114: 1036-1048.

URS Corporation. 2004. Hydraulic model of the Merced River Dredger Tailings Reach. Prepared for Stillwater Sciences, Berkeley, California.

Vick, J. C. 1995. Habitat rehabilitation in the lower Merced River: a geomorphological perspective. Master's thesis. University of California, Berkeley.

8 FIGURES

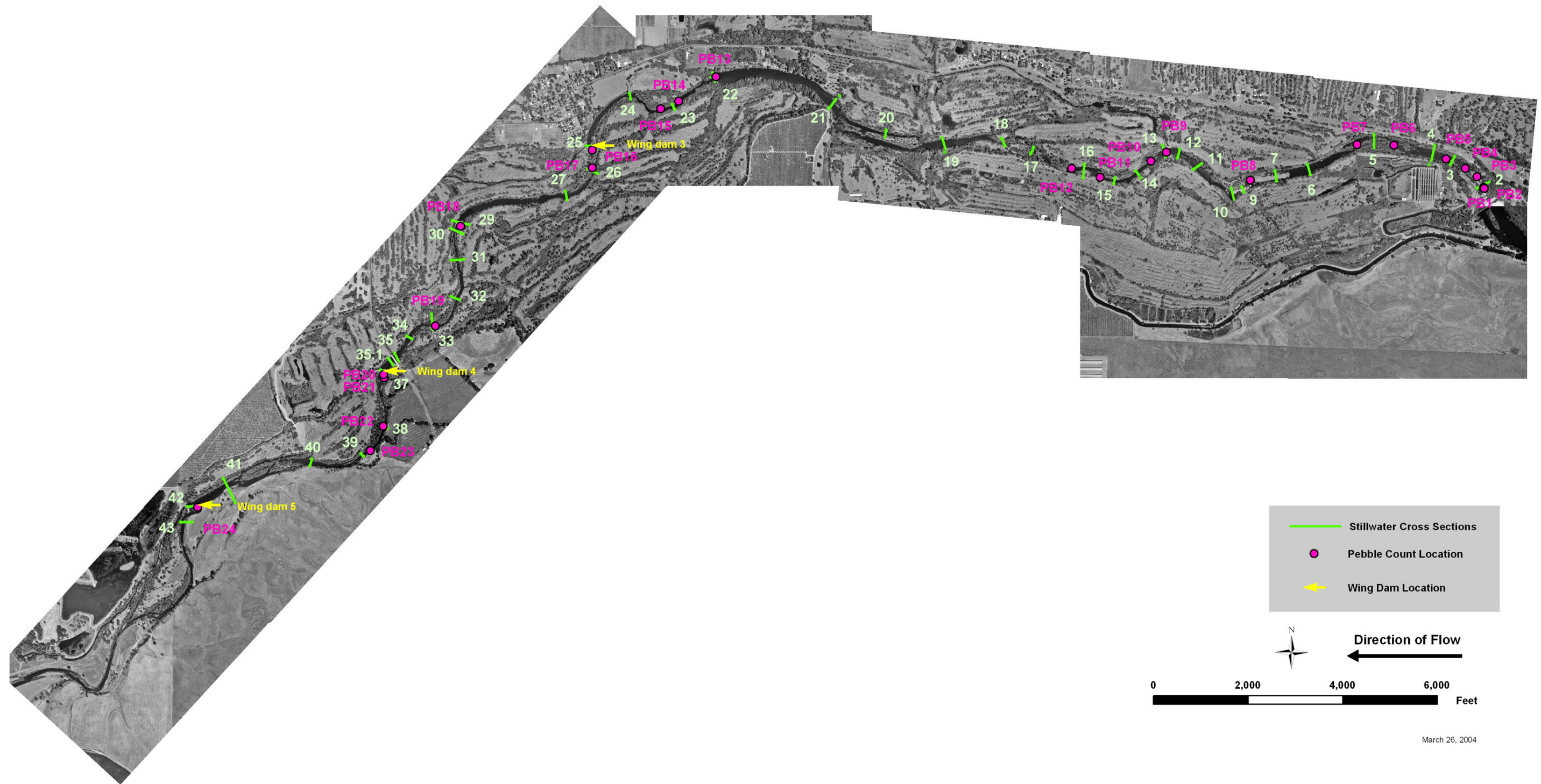


FIGURE 1
The Merced River Dredger Tailings Reach, showing locations of channel cross-section surveys, pebble counts, and wing dams. Unit conversion: 1,000 ft = 0.30 km.

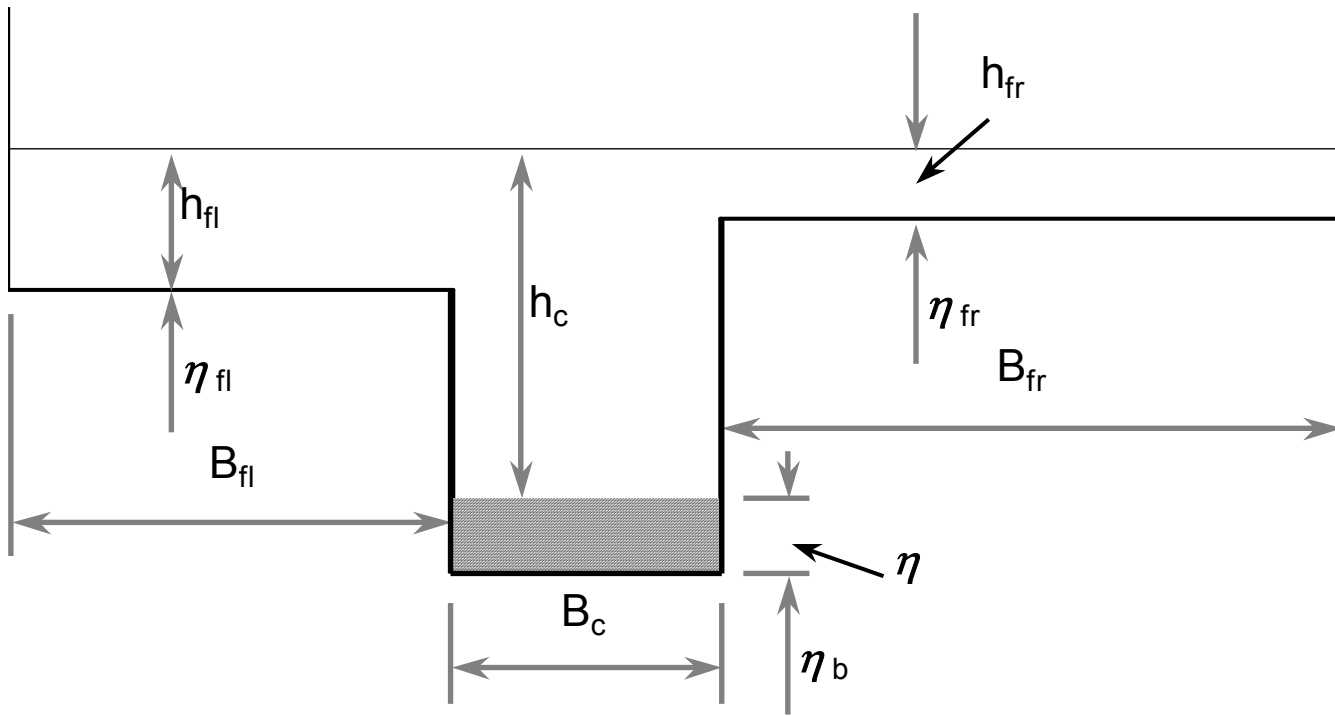


FIGURE 2
Simplified channel cross-section and definition of geometric parameters.

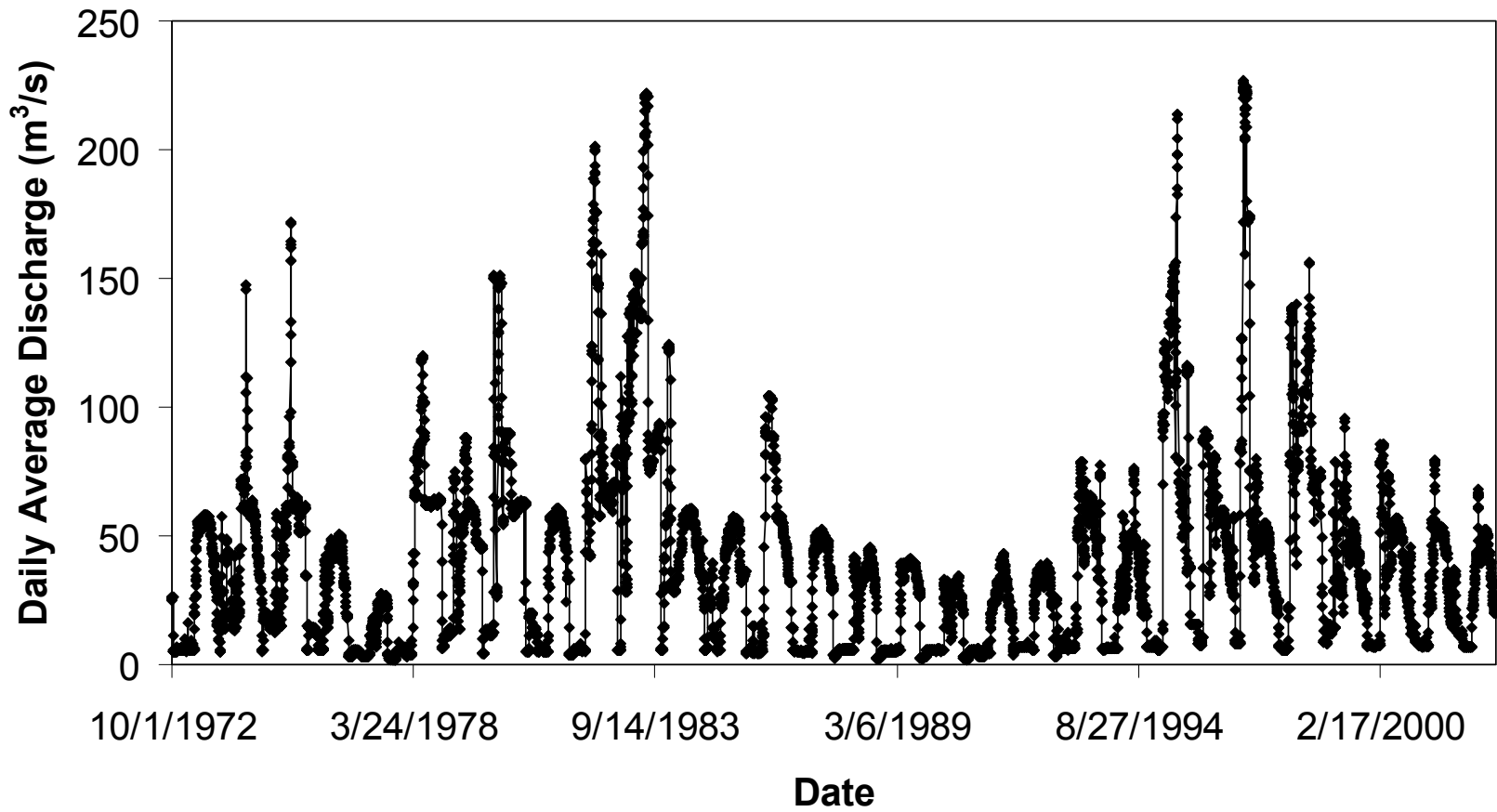


FIGURE 3

Daily average discharge record at the Merced River below Merced Falls Gauge (USGS # 11270900) for the post-New Exchequer Dam period between 10/1/1972 and 9/30/2002. Unit conversion: 1 m³/s = 35 cfs.

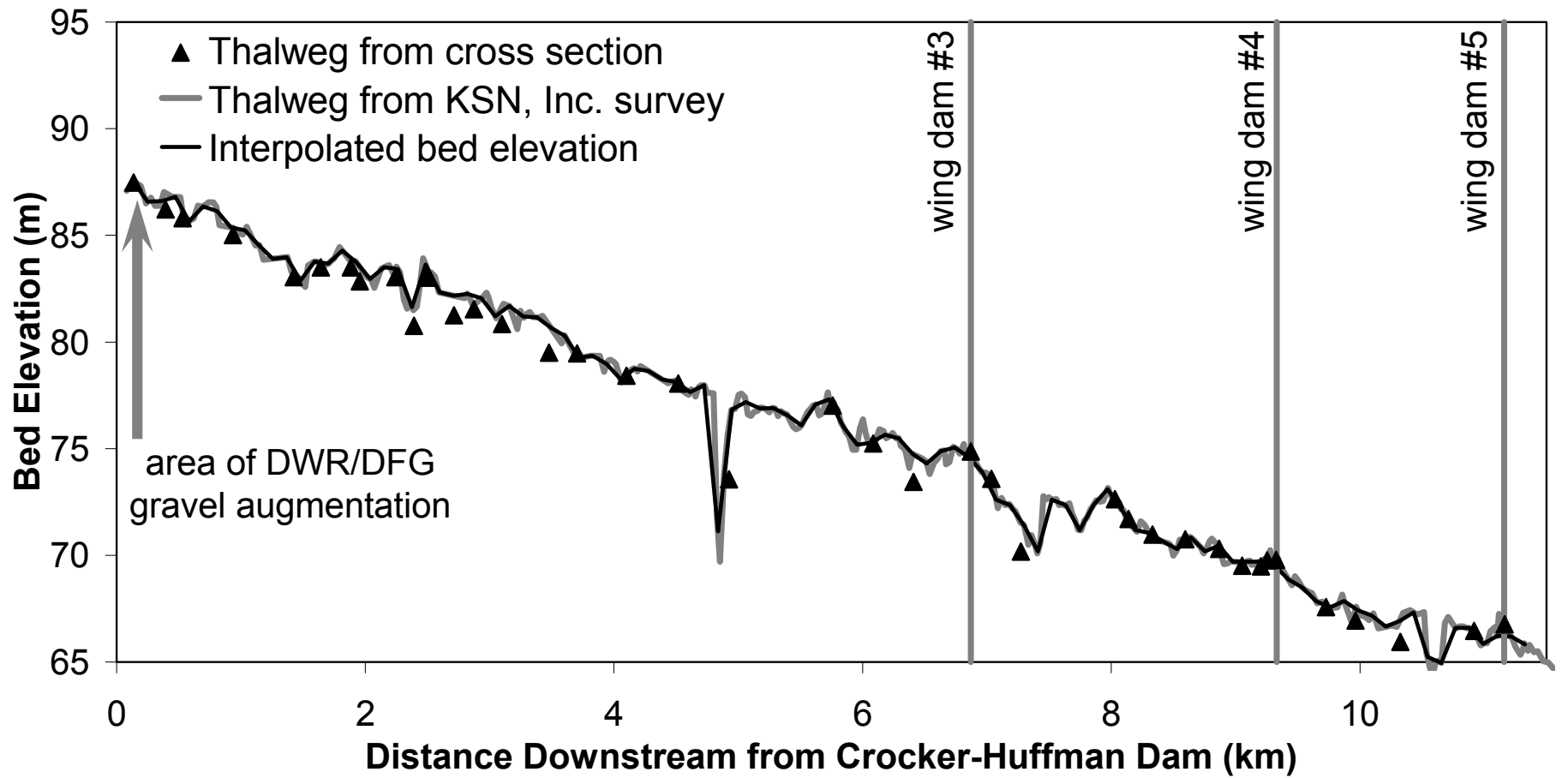


FIGURE 4

Longitudinal profile of the Merced River Dredger Tailings Reach. Interpolated bed elevations are based on KSN, Inc. survey data. Unit conversion: 1 m = 3.28 ft, 1 km = 0.62 mile.

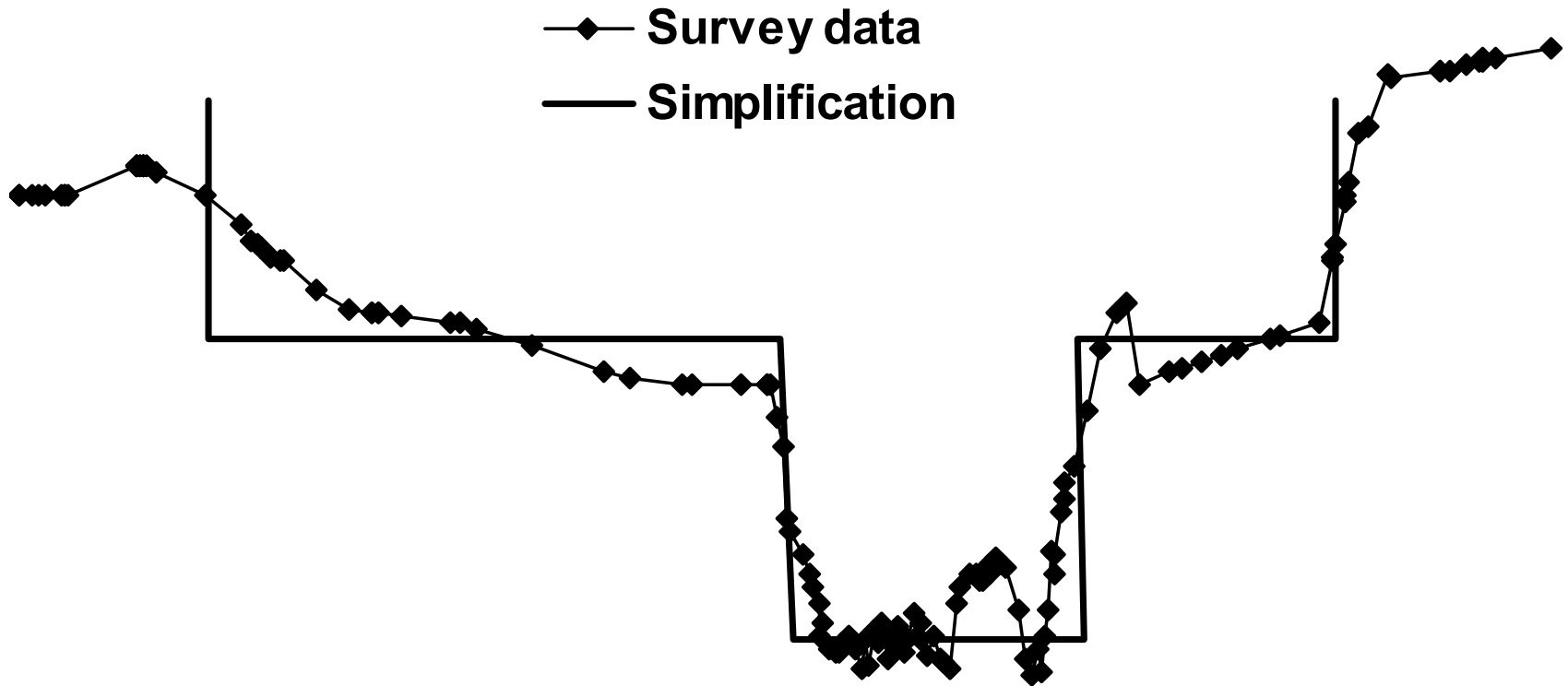


FIGURE 5
Simplification of surveyed channel cross-section. Survey data collected by Stillwater Sciences.

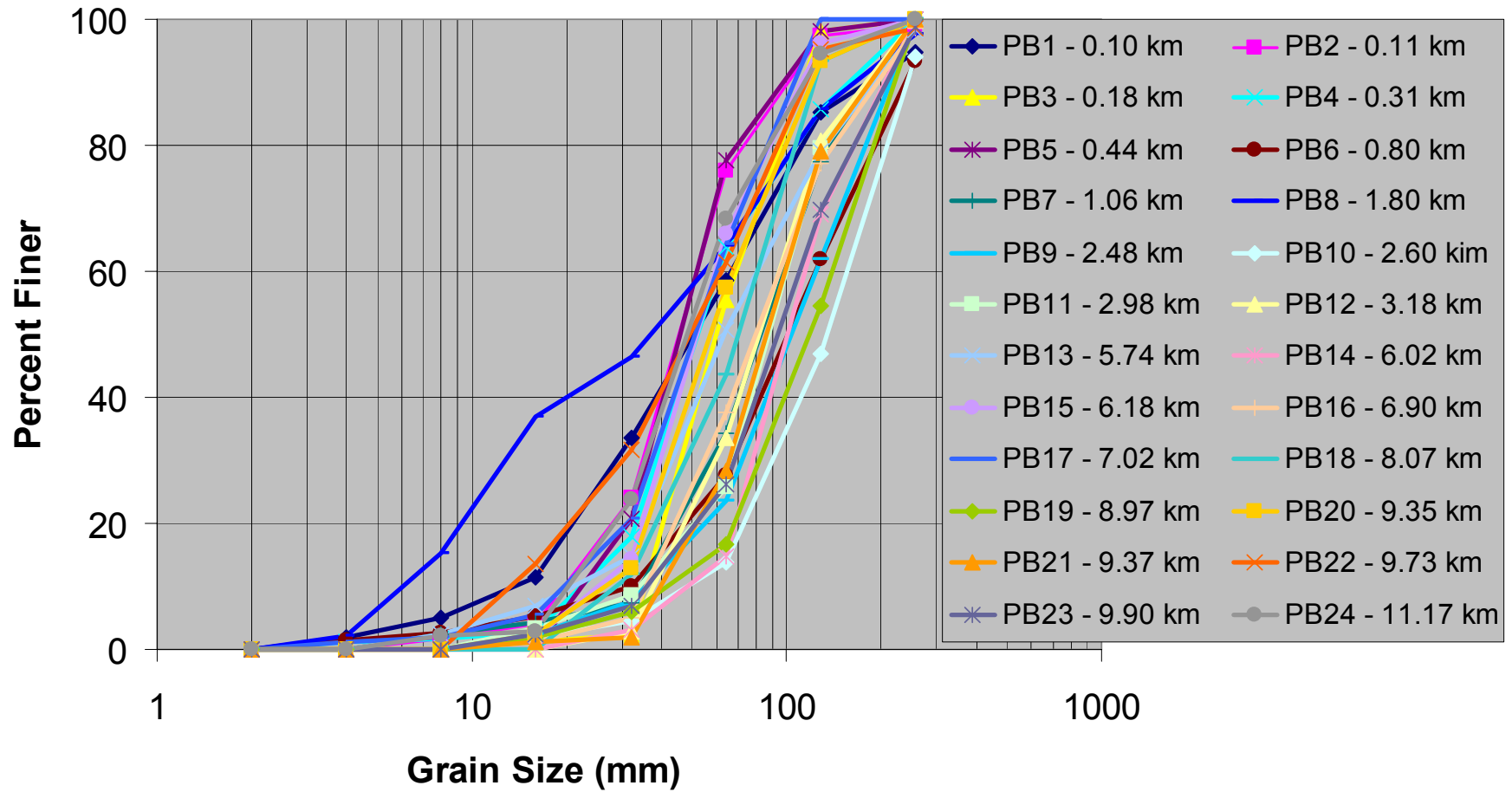


FIGURE 6

Pebble counts in the Merced River Dredger Tailings Reach, collected by Stillwater Sciences. Pebble count locations are provided as distance downstream from Crocker-Huffman Dam.

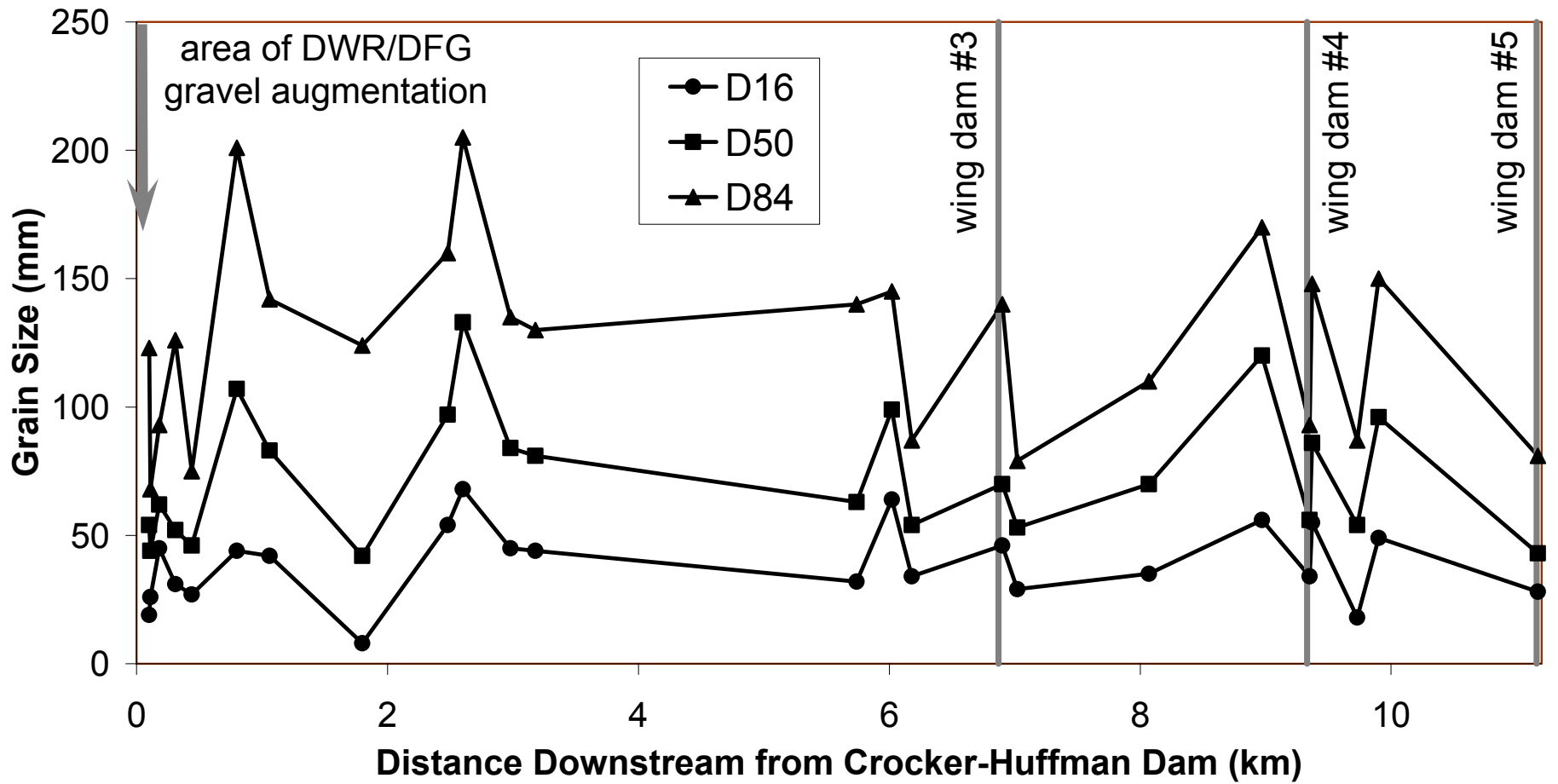


FIGURE 7

Characteristic grain sizes in the Merced River Dredger Tailings Reach. Unit conversion: 1 km = 0.62 mile.



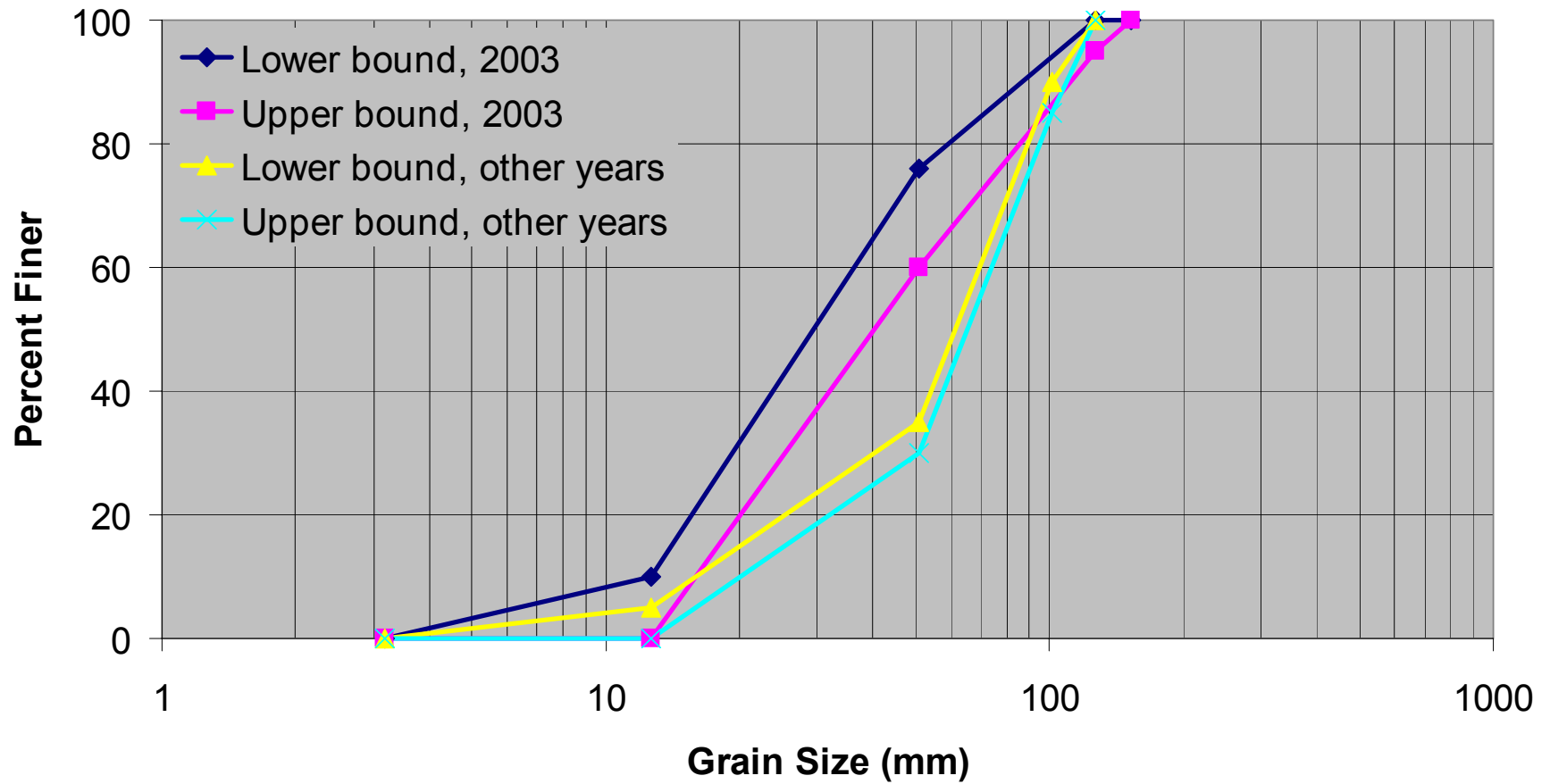
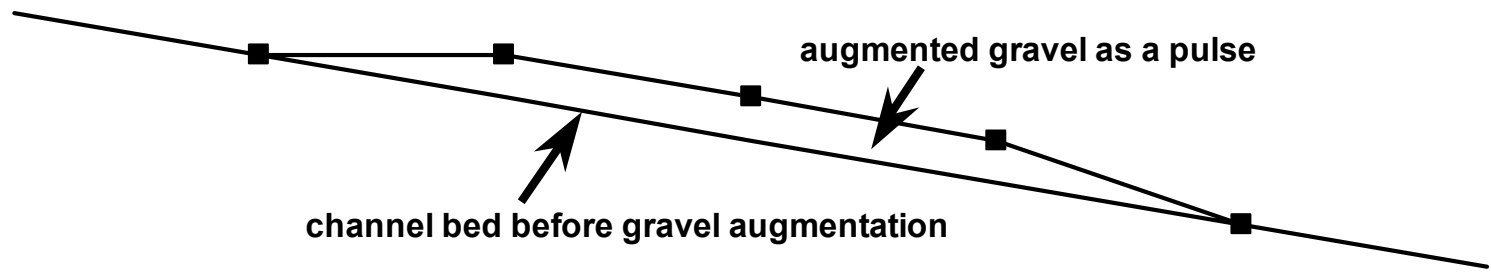


FIGURE 9

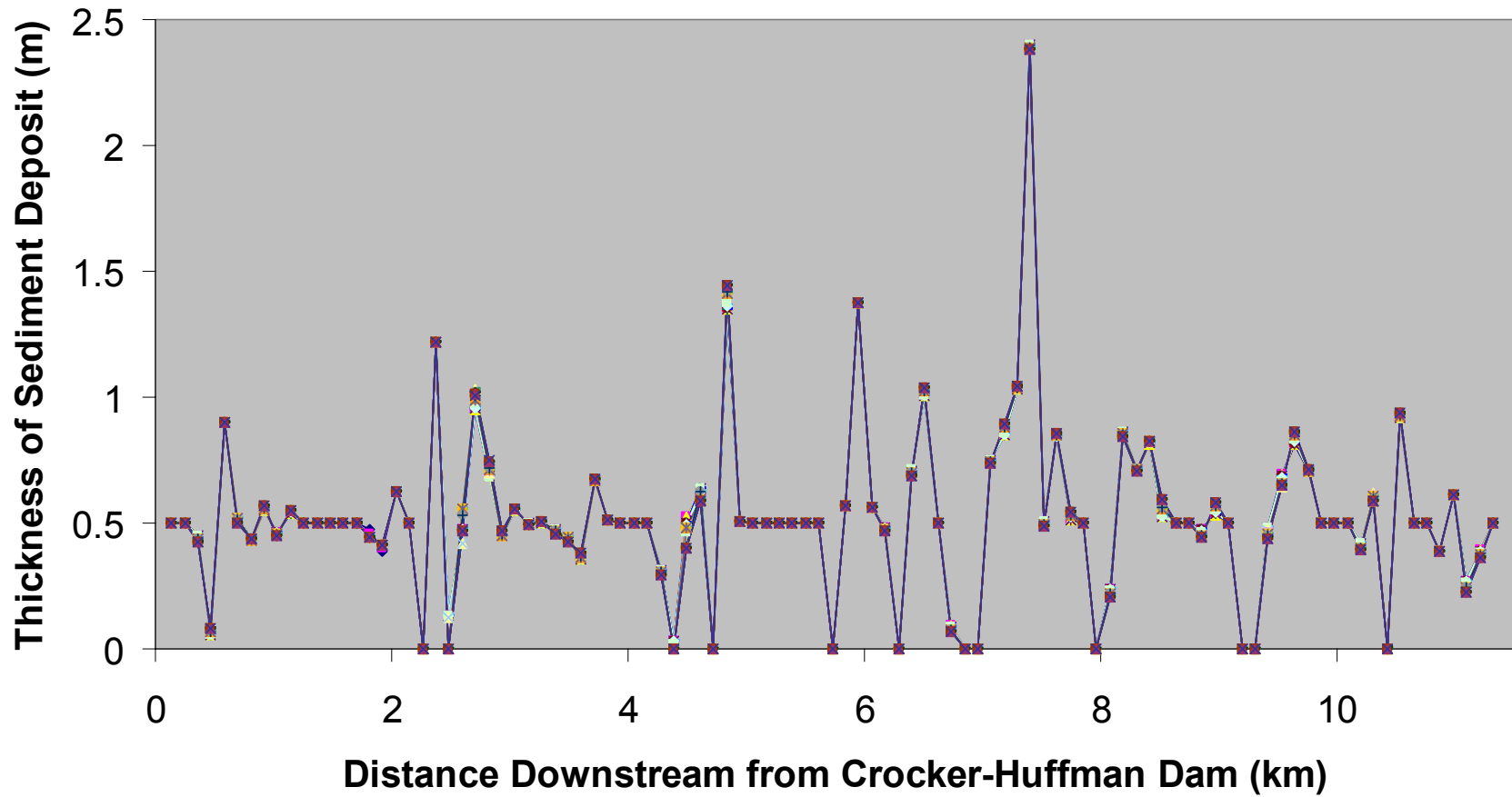
Estimated grain size distribution of gravel used at the Merced River Hatchery augmentation riffle. Source: Kevin Faulkenberry (pers. comm.).



augmented gravel as a pulse

channel bed before gravel augmentation

FIGURE 10
Sketch demonstrating the longitudinal distribution of augmented sediment as a gravel pulse.

**FIGURE 11**

Simulated thickness of sediment deposit for a 30-year period plotted annually, showing almost no change in bed elevation. No attempt is made in this diagram to show the thickness of individual years. Unit conversion: 1 m = 3.28 ft, 1 km = 0.62 mile.

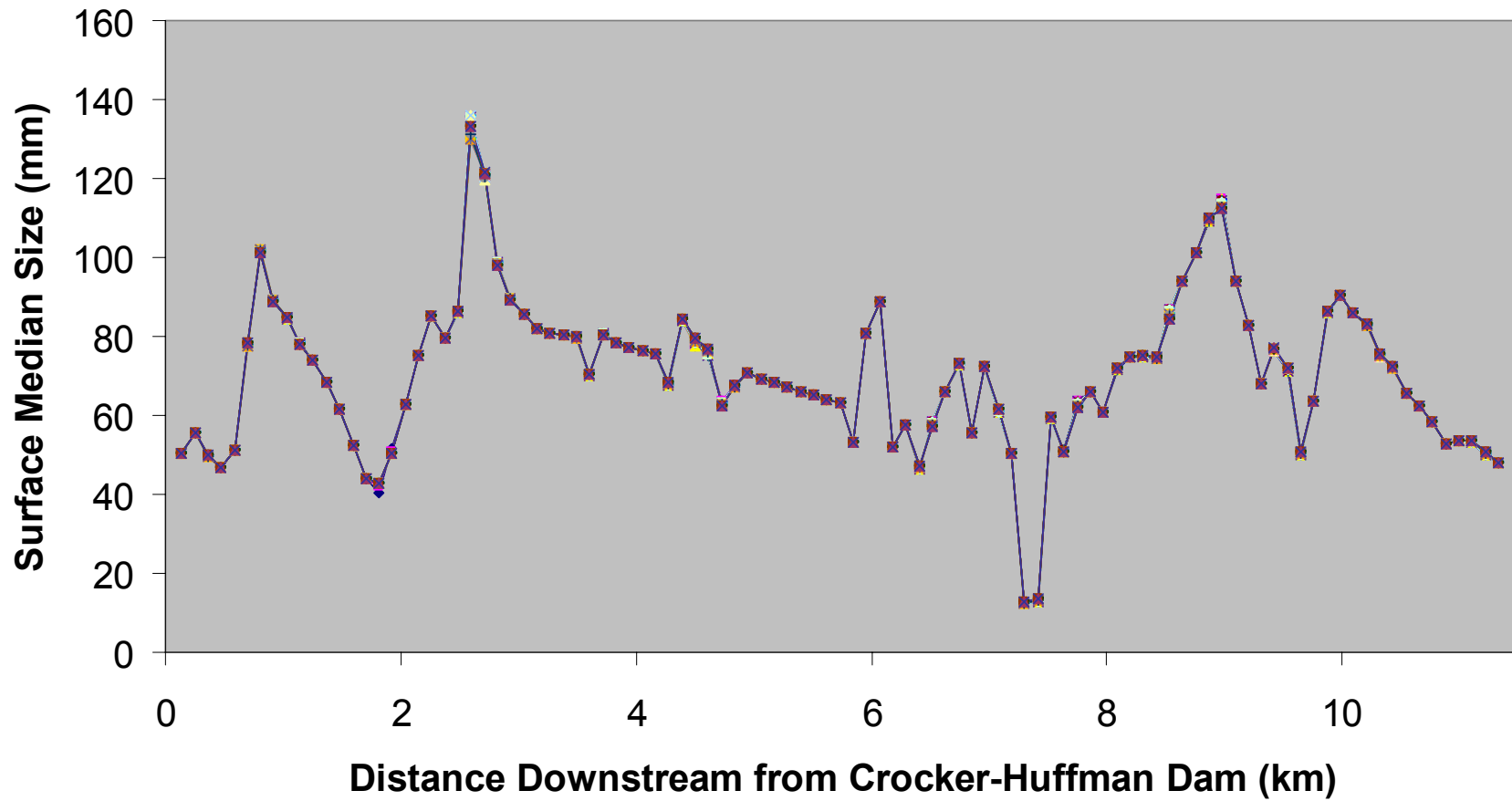


FIGURE 12

Simulated surface median size for a 30-year period plotted annually, showing that there is almost no change in bed texture. No attempt is made in this diagram to show the surface median size of individual years. Unit conversion: 1 km = 0.62 mile.

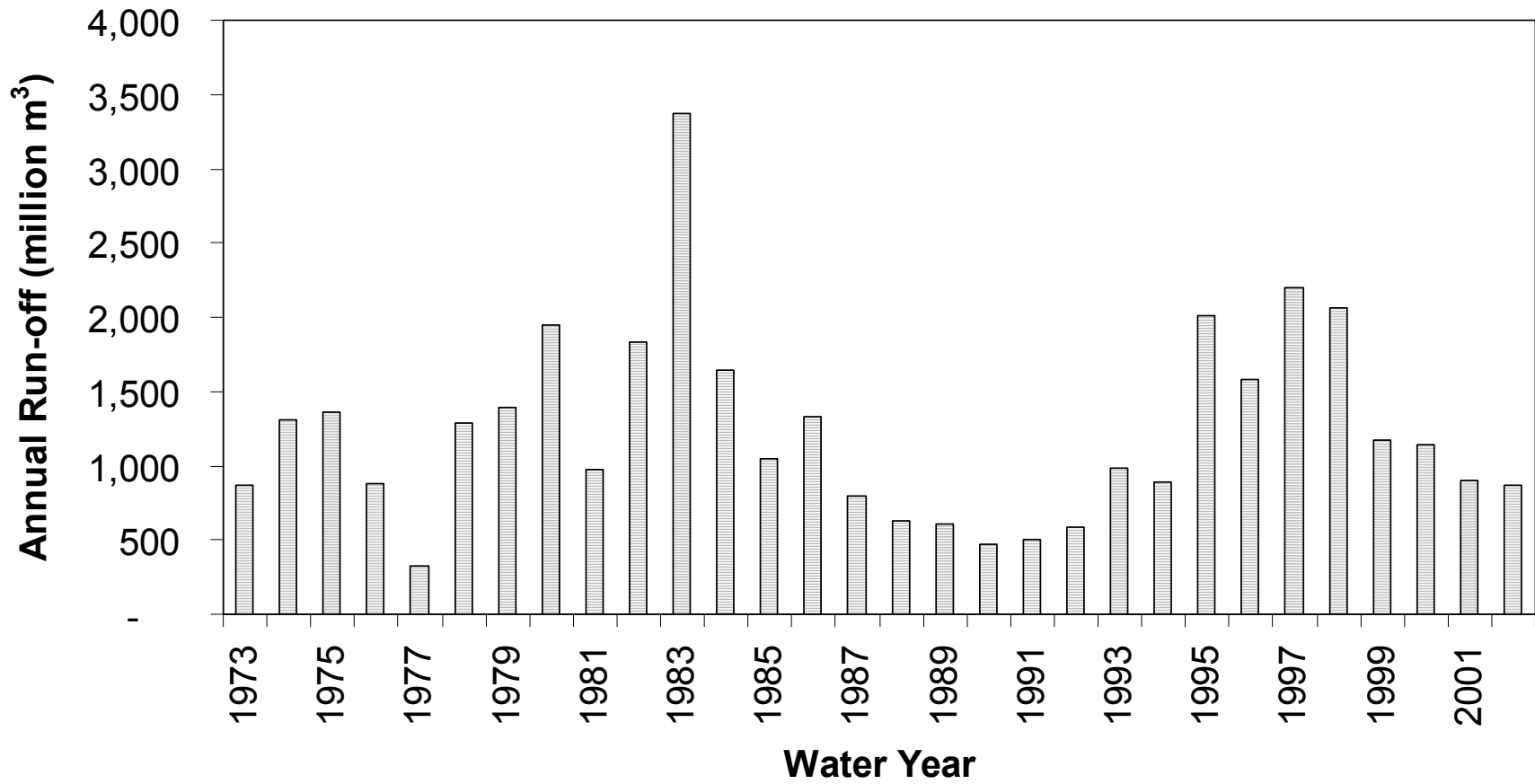


FIGURE 13

Annual run-off for the post-New Exchequer Dam period between water years 1973 and 2002, showing the wettest conditions occurring during water year 1983. Unit conversion: 1 million m³ = 810 acre-ft.

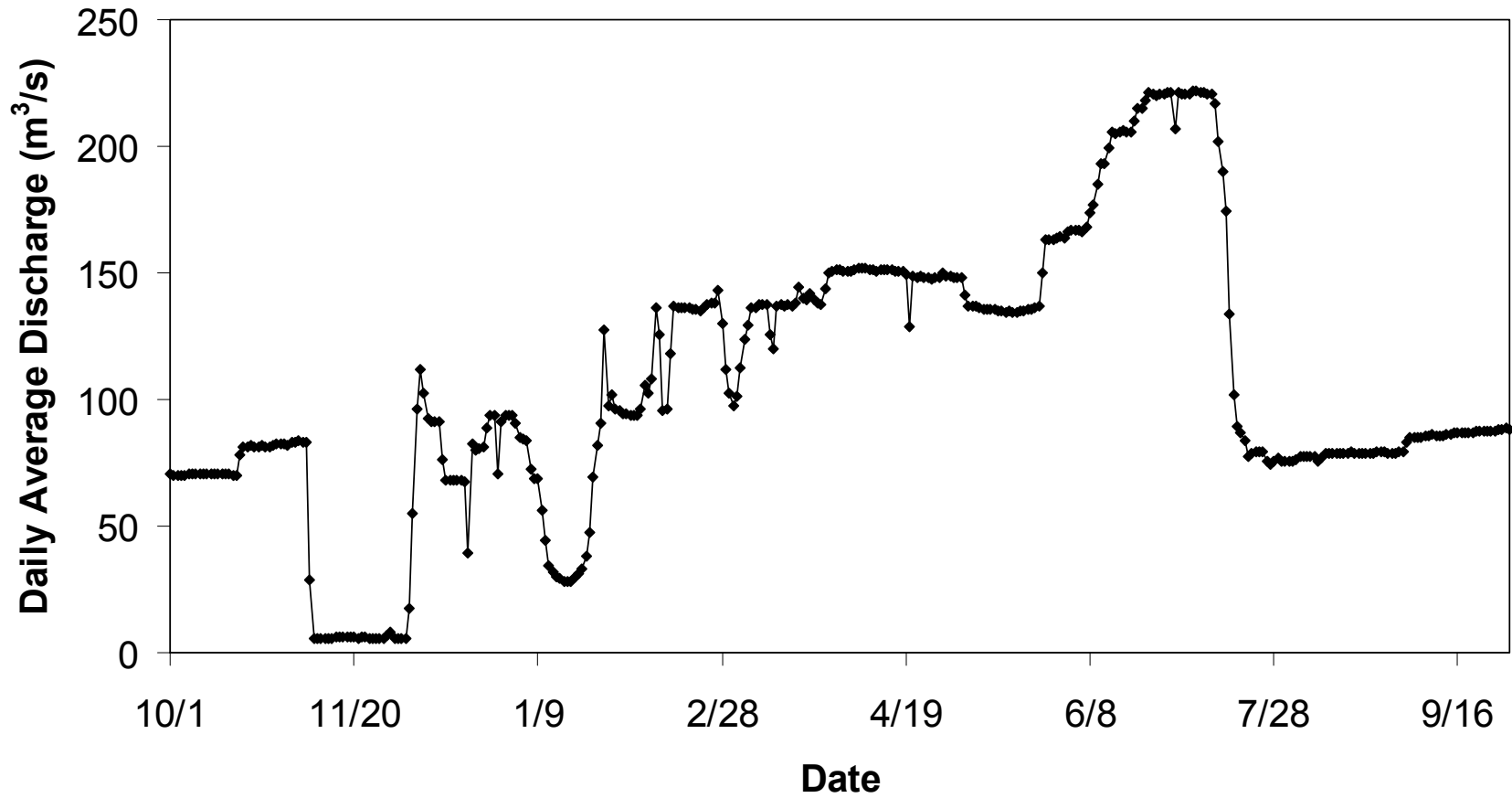


FIGURE 14

Daily discharge record for water year 1983, the wettest water year for the post-New Exchequer Dam period between water years 1973 and 2002. Unit conversion: 1 m³/s = 35 cfs.

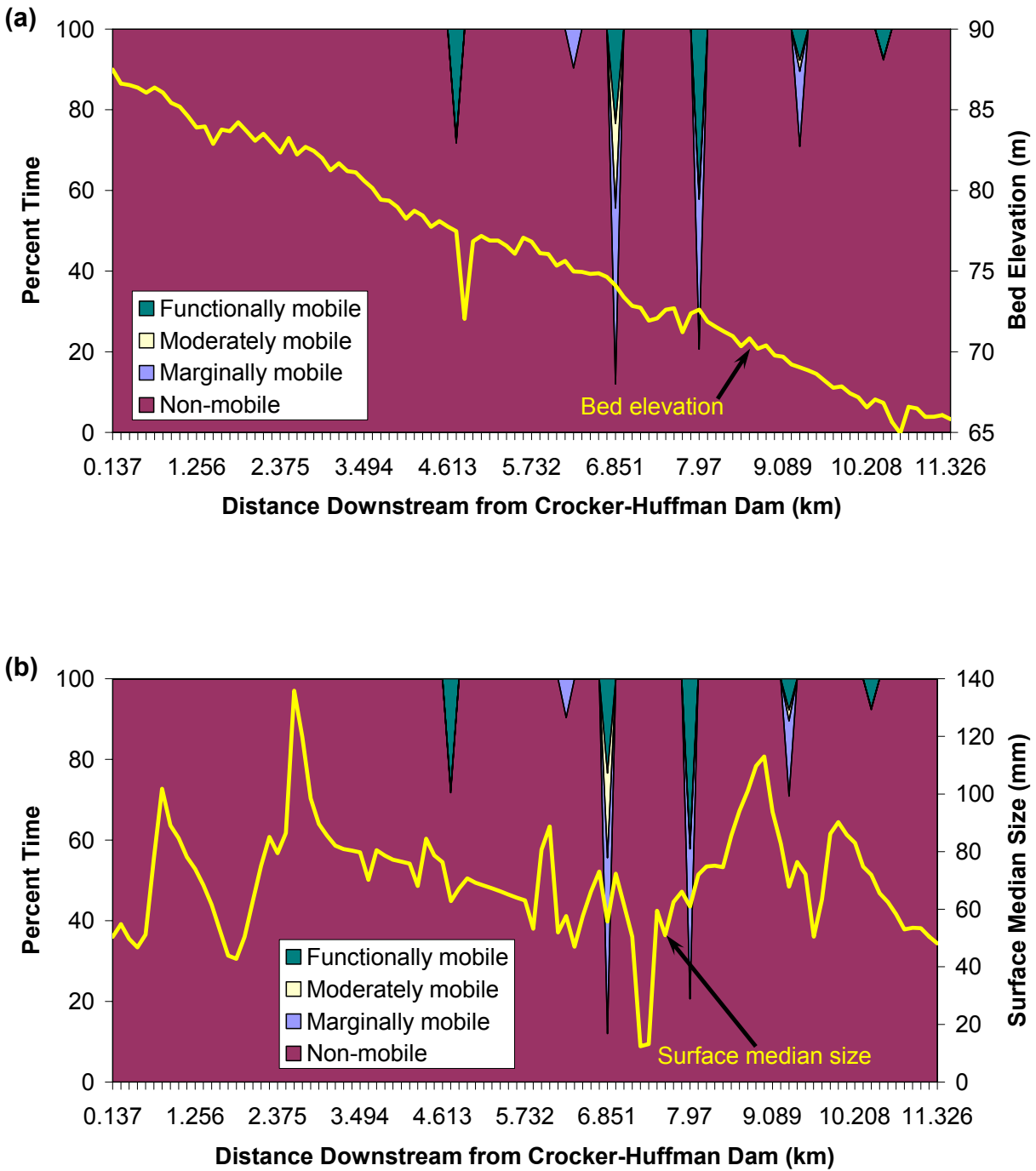


FIGURE 15
 Simulated bed mobility for water year 1983 in comparison with
 (a) river longitudinal profile; and (b) surface median grain size.
 Unit conversion: 1 m = 3.28 ft, 1 km = 0.62 mile.

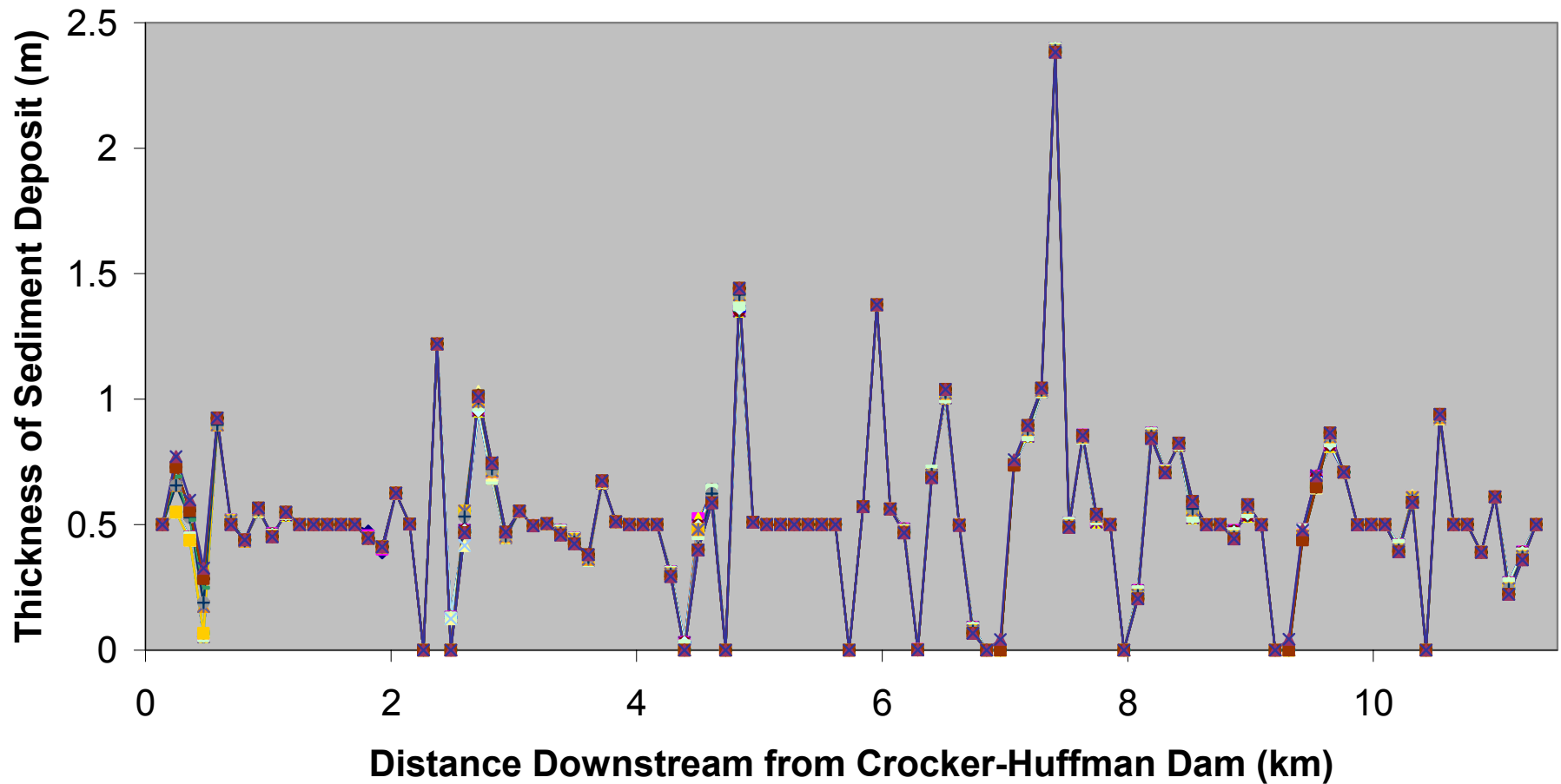


FIGURE 16

Simulated thickness of sediment deposit with the ongoing gravel augmentation before 9/30/2002, showing small but visible changes in bed elevation a short distance downstream of Crocker-Huffman Dam. Rather than differentiating the thickness of sediment deposition in different years, this diagram demonstrates that some changes in certain areas had occurred due to gravel augmentation. An example of the change in elevation due to gravel augmentation is detailed in Figure 18. Unit conversion: 1 m = 3.28 ft, 1 km = 0.62 mile.

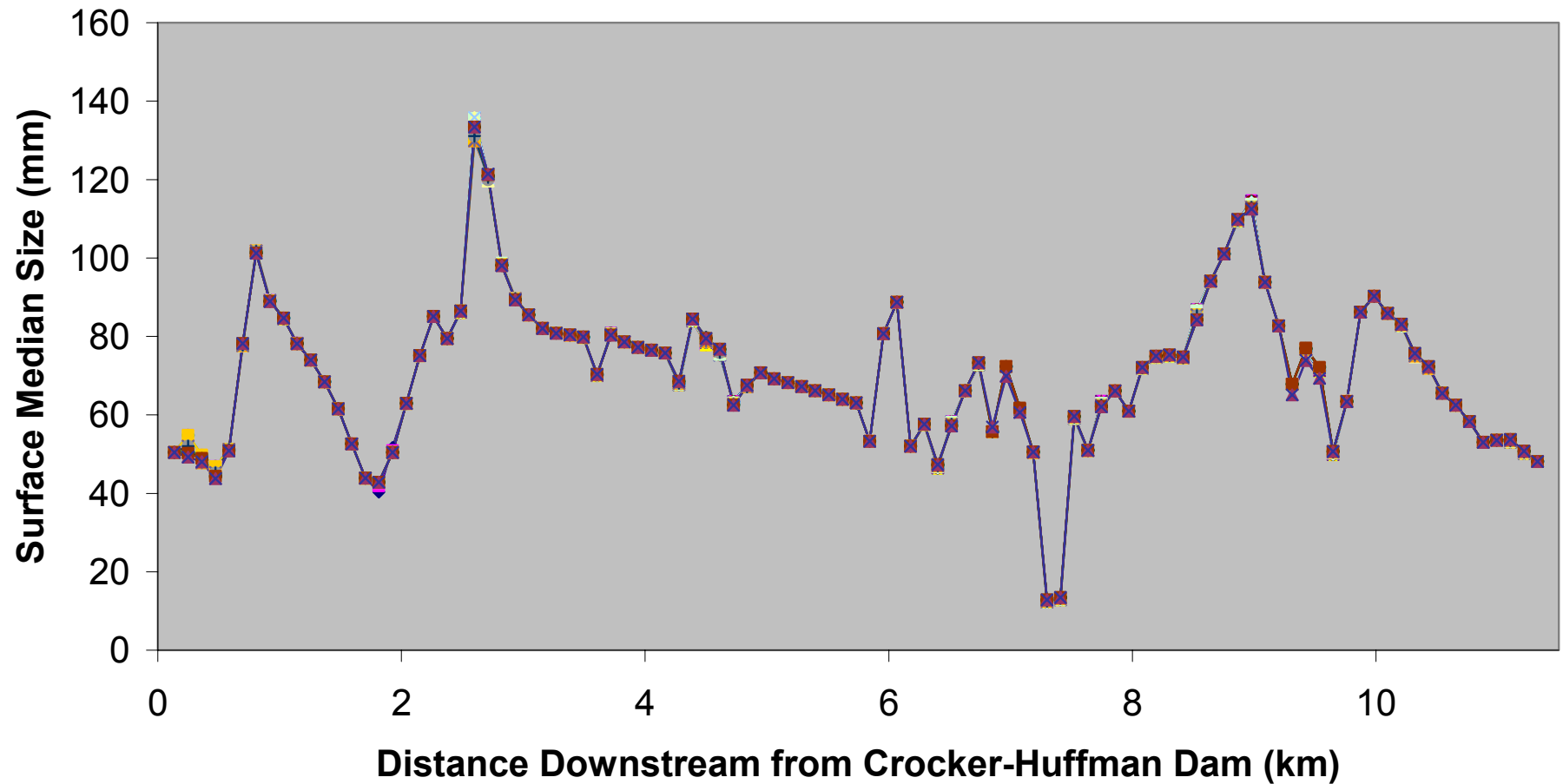
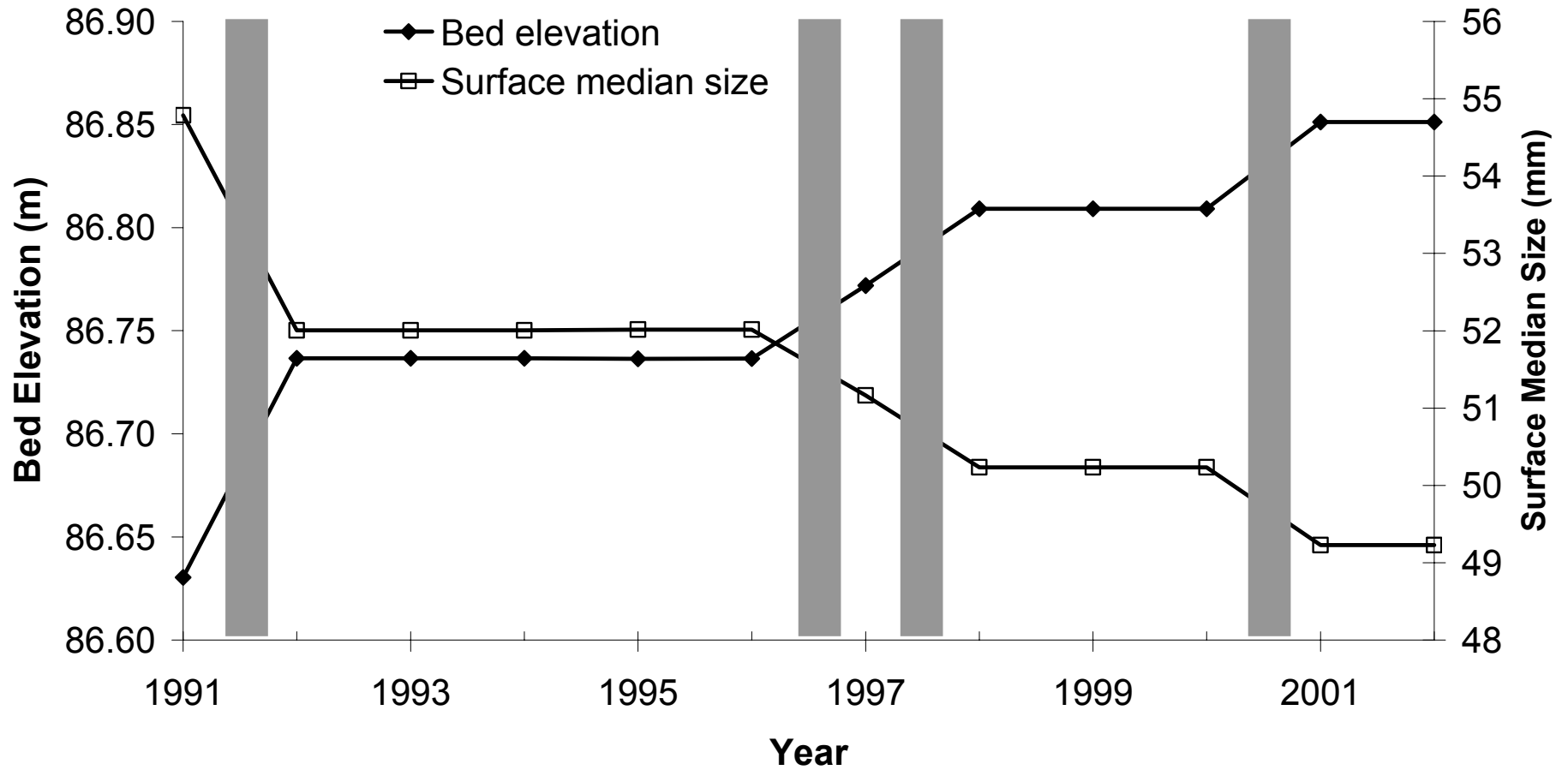


FIGURE 17

Simulated surface median grain size with the ongoing gravel augmentation before 9/30/2002, showing very small changes in grain size within a short distance downstream of Crocker-Huffman Dam. Rather than differentiating surface median size in different years, this diagram demonstrates that some changes in certain areas had occurred due to gravel augmentation. An example of the change in surface median size due to gravel augmentation is detailed in Figure 18.

Unit conversion: 1 m = 3.28 ft, 1 km = 0.62 mile.

**FIGURE 18**

Bed elevation and surface median size downstream of the hatchery gravel augmentation site approximately 250 m (820 ft) downstream of Crocker-Huffman Dam. The thick vertical bars indicate episodes of gravel augmentation at the site. The lack of appreciable change in bed elevation and median grain size between 1992 and 1996 following the 1991 augmentation, and between 1998 and 2000 following the 1997 augmentation, indicates the minimal transport capacity of the river. Unit conversion: 1 m = 3.28 ft.